



NTNU – Trondheim
Norwegian University of
Science and Technology

Seismic Forward Modeling of Deltaic Sequences

Ole-Peter Sæther

Master of Science in Engineering and ICT

Submission date: June 2013

Supervisor: Ståle Emil Johansen, IPT

Norwegian University of Science and Technology
Department of Petroleum Engineering and Applied Geophysics

Summary

The seismic forward modeling is a useful tool to predict the seismic response from a known geological model. A seismic forward modeling process contains two main steps, a model building step and a seismic forward realization part. The geological model may be built from scratch or an interpretation of some real seismic might be used as an input to the forward seismic realization algorithm.

In this work both the steps in a seismic forward modeling process are done. The first step is to build the geological model, which is based on an outcrop study from Storvola. Storvola is located alongside Van Keulenfjorden in the Central Basin on Svalbard. The sediments are from late Paleocene and Eocene time and are deposited from west to east.

The Deltaic section exposed at Storvola has been buried and undergone high pressure, deformation and faulting. The purpose of this study was to reverse this deformation by flattening the model so it represents a newly deposited delta.

An outcrop study has been performed by Johansen et al. (2007) in this area, where the exposed layers have been mapped and the properties have been measured. The mapped geology was digitized by using the software Petrel. The model building was based on the digitized data which the property models could be built out of. The three property models were the P-velocity, S-velocity and density. These properties were exported to the ECLIPSE file format which again was converted to the RSF format.

The second step in the seismic forward modeling process is the seismic realization. The open source software Madagascar is used to simulate a seismic survey, which predicts the responses from the subsurface by solving the center finite difference discretization of the elastodynamic equations. These equations use the property models as input. As a source a Ricker wavelet with a maximum spectre frequency of 100 Hz was used.

The resulting synthetic seismic gets re-sampled to reduce the amount of data and to speed up the processing, but carefully to not remove important data. Unwanted signals are removed or muted from the re-sampled data like the direct arrival. Common midpoint gathers are generated to simplify the generation of pictures of the subsurface before the data becomes migrated. The migration algorithm used is the 2-D prestack Kirchhoff time migration, which moves the reflectors to their correct position.

The migrated data is interpreted and compared to the original geological model. Almost all the thick layers with a high velocity contrast could be recognized, but some visualization problems were detected in areas with many thin layers.

Sammendrag

Fremover seismisk modellering er et nyttig verktøy for å forutsi seismiske responser fra en kjent geologisk modell. En fremover seismisk modellerings prosess inneholder to hovedsteg, et steg hvor modellen blir bygget og en seismisk simulerings del. Den geologiske modellen kan bli bygget fra grunnen av eller en tolket modell fra ekte seismikk kan bli brukt som input til simuleringsalgoritmen.

Begge stegene i fremover seismisk modellering ble utført i dette arbeidet. Først ble en geologisk modell bygget, og modellen var basert på blotningen av Storvola. Storvola befinner seg langs Van Keulenfjorden i Sentralbassenget på Svalbard. Sedimentene kom fra vest og ble avsatt mot øst tidlig i epoken tertiær.

Den deltaiske sekvensen som Storvola blottlegger har vært begravd og har vært utsatt for høyt trykk, deformasjon og forkastninger. Meningen med dette studiet har vært å reversere disse deformasjonene ved å flate ut modellen slik at den representerer et nylig avsatt delta.

En felt undersøkelse har tidligere vært utført av denne blotningen, hvor de synlige lagene ble kartlagt og egenskapene ble målt. Den kartlagde geologien ble digitalisert ved å bruke programvaren Petrel. Med den digitaliserte geologien som utgangspunkt ble egenskapsmodeller bygget. De tre egenskapsmodellene som ble bygget er P- og S-bølge hastighetsmodeller samt en tetthetsmodell. Disse egenskapsmodellene ble konvertert til ECLIPSE sitt fil format før de ble konvertert videre til RSF formatet.

Det andre steget i fremover seismisk modellering er seismisk simulering. Programvaren Madagascar ble brukt til å simulere en seismisk undersøkelse, som forutsier responser fra undergrunnen ved å løse en senter finite difference diskritisering av de elastodynamiske ligningene. Disse ligningene tar egenskapsmodellene som input. Til kilde ble en Ricker bølge med maksimum spekter frekvens på 100 Hz brukt.

Den resulterende syntetiske seismikken ble forsiktig resamplet slik at ikke noe viktig data gikk tapt, dette for å redusere datamengden og for å få prosesseringen til å gå fortere. Uønskede signaler ble fjernet eller dempet, slik som direkte bølgen før dataen ble sortert til common midpoint for å gjøre visualiseringen lettere. Til slutt ble dataene migrert ved hjelp av migrasjonsalgoritmen 2-D prestack Kirchhoff migration som flytter reflektorene til deres riktige posisjon.

Den migrerte dataen ble tolket og sammenlignet med den originale geologiske modellen. Nesten alle de tykke lagene med høy hastighetskontrast kunne bli gjenkjent i seismikken, men noen visualiseringsproblemer ble oppdaget i områder med mange tynne lag.

Acknowledgement

I would first of all thank my supervisor, professor Ståle E. Johansen, for the help, understanding, comments, feedback and insight he gave me through these past months. I also appreciate his assistance in writing this thesis both regarding to the guidance and correction.

In addition I would like to give a special thanks to professor Børge Arntsen and the PhD Candidate Espen Birger Raknes for their expertise, patience and assistance when it came to the software Madagascar.

I would like to thank Eli Kristine Austrheim, Knut Gunnar Steinsbø and Aleksander Engås for their assistance and discussion through this project. A special thanks goes to my good friend Simen Nygaard for getting me up early every morning through the last months and for his positive thinking and motivating talks. Thanks to Henriette L. Strømme, who sacrificed some of her time to read and make comments and corrections to this thesis, I appreciate it.

Table of Contents

Summary	i
Sammendrag	i
Acknowledgement	iii
Table of Contents	vi
List of Tables	vii
List of Figures	x
Abbreviations	xi
1 Introduction	1
1.1 Background and Purpose	1
1.2 Outcrop Study	2
1.2.1 Digital Data Acquisition	2
1.2.2 Fieldwork	2
1.2.3 Geologic Setting	3
1.3 Seismic Forward Modeling	3
1.3.1 Building a Model	5
1.3.2 Seismic Modeling Theory	6
2 Model Building	13
2.1 Background Material	13
2.2 Building a model in Petrel	14
3 Converting	19
3.1 Convert the geological model from Petrel to Madagascar	19

4	Seismic Modeling	21
4.1	Madagascar software	21
4.2	Stability	23
4.3	Seismic Modeling	24
5	Seismic Processing and Interpretation	27
5.1	Processing	27
5.1.1	Re-sample	27
5.1.2	Mute	29
5.1.3	Sort into Common Midpoint - gather	29
5.1.4	Velocity Analysis	30
5.1.5	Migration	31
5.2	Interpretation of the Synthetic Seismic	34
6	Discussion	37
6.1	Model Building	37
6.2	Generation of the Synthetic Seismic	37
6.3	The Interpretation	38
6.4	Data Quality	39
6.5	Comparison of the Synthetic Seismic and the Geological Model	40
7	Conclusion and Recommendation	43
7.1	Conclusion	43
7.2	Further Work	43
	Bibliography	45
	Appendix	I
	Appendix A - Pictures	I
	Appendix B - Model building in Petrel	XIII
	Appendix C - Converting a Petrel model to Madagascar	XIX
	Appendix D - Seismic Acquisition	XXIII
	Appendix E - Processing	XXV

List of Tables

1.1	Digital data collection methods and their properties	2
2.1	Geophysical values used in the property models	17
4.1	Acquisition parameters	25
C.1	Output files from Petrel	XX

List of Figures

1.1	Early paleocene surface map	4
1.2	How an incident P-wave is divided according to Snell's law	7
1.3	How an incident P-wave at critical angel behaves according to Snell's law	7
1.4	Illustration of ray tracing	8
1.5	Illustration of the center-difference	9
2.1	Picture of the outcrop Storvola	13
2.2	Geological model of Storvola and the surroundings	14
2.3	P-velocity model of Storvola	15
2.4	Picked horizons on a picture in Petrel	15
2.5	Moving surfaces	16
2.6	P-velocity model built in Petrel	17
3.1	Illustration of the RSF file format	19
3.2	Converted P-velocity model	20
4.1	Resized figure 3.2	23
4.2	The Ricker wavelet and its specter	24
4.3	Wave field	24
4.4	Acquisition positions	25
5.1	Common Shot Gather	28
5.2	A Muted Shot	28
5.3	Common Midpoint gather	29
5.4	Common Midpoint gather geometry	30
5.5	RMS-velocity model	31
5.6	Kirchhoff time migration	32
5.7	The migrated data	33
5.8	Interpret Seismic - Greyscale	34
5.9	Interpret Seismic - Red-white-blue	35
5.10	Visible layers in the seismic	35

6.1	Data Quality	39
6.2	Grid problems	40
6.3	Model versus synthetic seismic	41
A.1	Large picture of figure 2.6	II
A.2	S-velocity model built in Petrel	III
A.3	Density model built in Petrel	IV
A.4	Large picture of figure 3.2	V
A.5	Converted S-velocity model	VI
A.6	Converted density model	VII
A.7	Large picture of figure 4.1	VIII
A.8	Large picture of figure 5.8	IX
A.9	Large picture of figure 5.9	X
A.10	Large picture of figure 5.10	XI
A.11	Large picture of figure 6.3	XII
B.1	V-velocity model of Storvola	XIII
B.2	Mapped layer in Petrel on a picture	XIII
B.3	Make/edit surface and smoothing process	XIV
B.4	Generated surface	XV
B.5	Moving surfaces	XV
B.6	Surface calculator and Geometrical modeling process	XVI
B.7	Final surfaces	XVI
B.8	Built V_p -property model	XVII
C.1	Illustration of the RSF file format	XIX
C.2	Converted P-velocity model	XXI

Abbreviations

FD = Finite difference
CMP = Common Midpoint
RMS = Root Mean square

Introduction

1.1 Background and Purpose

Seismic forward modeling is a useful tool to explore seismic responses from different sources and receiver setups over an identical geological model. The reason why seismic forward modeling is used in addition of traditional seismic surveys is because it saves time and money. It is possible to save a lot of money when a computer, or rather a cluster of computers, do the work instead of a fully crewed seismic vessel. A seismic vessel needs to do a new survey for every setup property. A cluster of computers has the possibility to run different acquisition setups simultaneously over the same area (how many depends on the size of the cluster and the acquisition size). The resulting synthetic seismic from all of the different acquisition setups are available much faster and a decision for the acquisition parameters used in the real data acquisition can be determined, hence money saved. The synthetic seismic is just a prediction of what may be in the subsurface. A real seismic acquisition has to be executed in any case. The synthetic seismic can never replace real seismic, only help understand it.

This master thesis builds on the work done by Johansen et al. (2007) on the outcrop of Storvola. Storvola is a well documented outcrop in Van Keulenfjorden on southern Svalbard in the Norwegian Arctic. The geology of Storvola is a deltaic section from Eocene time and consists of turbidites, marine shale, delta-slope and delta-front deposits and, at the top, coastal plain deposits.

This deltaic section has been buried and undergone high pressure, deformation and faulting. The purpose of the study is to reverse the deformation and get a geological model that represents a newly deposited delta. This model is used to produce synthetic seismic, which is interpreted and compared to the geological model. This delta is also comparable to sections in the Barents Sea and the study may give some clues to what is possible to detect using seismic in this area.

1.2 Outcrop Study

”By studying an exposed outcrop, such as a cliff section or quarry, geologists can get insights into the process that occurred at the time of deposition, and make quantitative measurements...” (Buckley et al., 2009)

When building a geological model out of a mountainside, the best way to get the model as correct as possible is to do an outcrop study. An outcrop study can be done in several ways, like using photogrammetry and fieldwork, but a combination of these methods gives a more reliable model. The photogrammetry gives the geological structure and the fieldwork verifies the photogrammetry. In addition fieldwork also give some properties parameters of the different rocks together with laboratory measurements.

1.2.1 Digital Data Acquisition

There are several methods to acquire the geological structure of an outcrop (see Table 1.1 for a selection of methods). The accuracy of these measurements spans from meters to some millimetres. In this project the ground-based photogrammetry is the method of interest, since this method was the one used by Johansen et al. (2007), but also GPS is very useful in the fieldwork stage.

”Ground-based photogrammetry software can be utilised where accuracy and precision are less important than speed and collection of large volumes of surveyed data.” (Pringle et al., 2006)

Ground-based photogrammetry uses high-resolution images from digital cameras taken from different locations of the outcrop. The images are combined to create an accurate digital photo of the whole outcrop. Software can also generate a surface model from these images and convert the surface model into a geographic coordinate system. The surface model can now be used to extract stratigraphic data but also to place field data (e.g. sedimentary logs and laboratory measurements) (Pringle et al., 2006).

Digital data method	Accuracy	Advantage	Disadvantage	Cost
Ground-based digital photogrammetry	0.1-0.5m	Fast	Medium time processing	Relatively cheap
Hand-held GPS	1-5m	Locational fix	Significant 'Z' positional error	Very cheap

Table 1.1: A selection of data collection methods and their properties, adapted from Pringle et al. (2006) page 35)

1.2.2 Fieldwork

Fieldwork is the basis for the understanding of the geology. The petrophysical properties are collected to help the geologist understand the geology. From each of these properties it is possible to build a property model. These models are difficult to get accurate because: ”the parameters vary in two dimensions within the model, any values assigned to a given layer must be considered an approximation” (Johansen et al., 2007).

Therefore rock samples from different layers are collected and sent to a laboratory for testing of density and velocities. Well data from similar geology can also be used to verify measured properties, but well data is not always available. It is also possible to use hand-held equipment and measure the properties directly, this to get a good overview of the properties in the different layers. Grain characteristics can also be acquired in fieldwork. This can tell if a layer may be a good reservoir rock or not and which processes the rock has undergone when buried. Porosity measurements are important if a layer in the outcrop is a target for production of oil or gas somewhere in the area, but also to get a more complete model which can be used in a comparison with well logs.

A hand-held GPS is a useful tool to place logging results and measurements in the right place in a geological model. A GPS is a necessary tool in fieldwork despite the large error it may have in the Z-direction (height) (Pringle et al., 2006).

1.2.3 Geologic Setting

The outcrop explored in this study is the outcrop of Storvola alongside Van Keulenfjorden on the southern Spitsbergen in the Norwegian Arctic. During early Tertiary an ocean spreading system developed and Svalbard cut off from Greenland. During this process the western parts of Spitsbergen were folded and thrust and a new mountain range was created. Within this uplift, a large directed bay had been formed, caused by a subsidence of the land surface. This is referred to as the Central Basin (see figure 1.1). The basin got filled by eroded material (Johnsen et al., 2001; Dallmann, 2009).

In the late Paleocene and Eocene time this infilling progressed from west to east and are now exposed alongside Van Keulenfjorden. The exposure at Storvola shows the progradation from marine shale via delta slopes and delta fronts, to coastal plain deposits (Johansen et al., 2007). The tectonic activity in the area caused slow, periodically flooding and regression of the sea (Dallmann, 2009).

1.3 Seismic Forward Modeling

Seismic forward modeling is seismic forward realization of a given geological model. (Alaei, 2012)

In seismic forward modeling there are two main steps, building the geological model and a numerical computation of the seismic response from the model. This means that the result of the seismic forward modeling is dependent on the building of the geological model just as much as the seismic forward realization method (Alaei, 2012). If the model building is poorly executed there are no seismic realization methods to fix this, hence a poor seismic result. It is also possible to have a well performed model building step, but if in the realization step wrong parameters has been used, the result will most likely be poor. Therefore is it important to quality control the work periodically, this might save a lot of time.

Seismic modeling is an important process in many aspects of exploration seismology because it increases the reliability of the seismic data analysis (Alaei, 2012). The application of seismic modeling in seismic acquisition is to reduce the risk in the seismic exploration and to design a better survey. If the geological setting is complex, seismic modeling

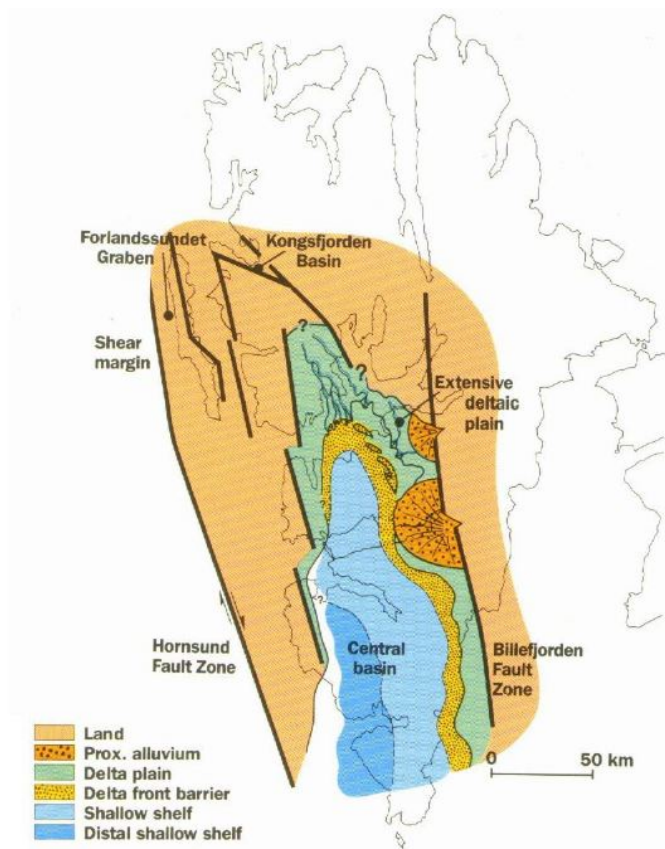


Figure 1.1: Surface map of the early paleocene time of Svalbard (from Johnsen et al. (2001)

can be used to test different acquisition parameters in the real seismic survey and obtain the optimal data quality. Prior to acquisition, seismic modeling can be used to ensure that the seismic signature of the geological objective of the survey will be seismically visible (Anderson and Cardimona, 2002).

In seismic processing, seismic modeling is used to test different processing algorithms and sequences. The migration sequence is one of the most important sequences to calibrate in seismic modeling.

Seismic interpretation may use seismic modeling to relate the response of an interpreted geologic model to real data. Seismic modeling may be used to investigate different problems that may appear during interpretation of real data. This verifies the interpretation, especially in complex areas. After the interpretation of real seismic data, the interpreted model can be used as input in seismic modeling. The generated synthetic seismic data can be compared to the real data by looking at the difference in responses. This can verify the geological model or it may invalidate the model. If so, the geological model can be altered before computing new synthetic seismic and compare again. This process may continue to the match is satisfactory between the synthetic and real data (Krebs, 2004).

1.3.1 Building a Model

Model building can be divided into two types, interface based models and grid based models. Both processes start with building the geometry of the model and continues by applying properties like velocities and density to the different layers of the model. When building the geometry of a complex model it is a good habit to start mapping the large structures before the small ones. The small details are important for the model to be as realistic as possible, because these details are important for the way the wave propagates.

Before building a model there are some questions that might be worth answering (Alaei, 2012). It may save a lot of time later in the process.

1. How large should the model be?
2. Should the model be 2D or 3D?
3. How complex should the model be?
4. What properties should the model contain, where should the values be obtained and how should they vary?

How to obtain the properties depends on the availability of data. In an outcrop study, fieldwork measurements and laboratory measurements might be the sources, in other studies sonic logs, checkshot surveys or Vertical Seismic Profile (VSP) data might give the property data. The velocity models are usually interval velocities, which is the thickness of the layer divided by the travel time through the layer.

Interface Based Models

The first step in an interface based model building is to decide the dimensions of the model. The next step is to fill the model with horizons and faults (interfaces). These interfaces are constructed by curves or lines. The curves consist of points in the time or depth domain. It is only necessary to pick some points along a horizon, an interpolation algorithm fills in the rest and generates the interface. When the geological model is constructed it is necessary to assign physical properties to the layers in the model. The seismic modeling needs the properties of the P-and S-wave velocities and the densities. These properties are assigned to blocks in the model, a block is defined as the intersection between different interfaces and/or the model boundaries. Interface based models are used in asymptotic seismic realization methods, which is described later.

Grid Based Models

Grid based models are represented by points called 'nodes'. These nodes are linked to their neighbors and form a grid. The grid is usually a structured grid which have the same distance between each point in the same direction. The distances between the points might be different in the the different dimensions, but normally the same distance between the points are used in all directions. This because it makes the equations easier to solve, and the computation time is smaller.

Every node has a coordinate value (x,y,z) and physical properties (density and velocity). When building a grid based model the technique is very similar to the one used in building an interface model. The first step is to define the size of the model and then map the geological structures within the model. Then assign properties to the units or, rather, assigning values to the nodes within the unit. Grid based models are used in direct seismic realization methods, which is described later.

1.3.2 Seismic Modeling Theory

The Seismic modeling methods calculate the seismic response from the subsurface model and record the responses with receivers. The methods look at the way the seismic waves propagates from the source, through the model and back to the receivers. The input to the seismic modeling is models with the required properties. It is also necessary to decide acquisition parameters like the source signal, which often is a Ricker wavelet. The two most common methods are asymptotic and direct methods and these are described later.

Snell's law

Before describing the methods, it is necessary to talk about Snell's law. Snell's law is much used when evaluating seismic responses from horizons and the equation is:

$$\frac{v_i}{\sin(\theta_i)} = \frac{v_r}{\sin(\theta_r)} = \frac{v_t}{\sin(\theta_t)} \quad (1.1)$$

where v is the wave velocity for a given layer, θ is the angle of the wave propagation compared to the normal of the given boundary. i , r and t are the incident, reflected and transmitted wave respectively.

Snell's law phrases that the incident angle equals the reflected angle if the velocities of the two waves are equal. On the other hand, if the velocity of the reflecting wave is different from the velocity of the incident wave the reflecting angle has to change. In an interface between two different substances the transmitted wave is bent (the propagation angle changes) since the properties of the substances are different.

When an incident wave reaches a certain angle, called the "critical angle", the transmitted wave propagates along the interface between the two substances (the transmitted wave has an angle of 90°). The equation for the critical angle is,

$$\theta_{cr} = \sin^{-1}\left(\frac{v_1}{v_2}\right) \quad (1.2)$$

where θ_{cr} is the critical angle and v_1 and v_2 are the velocities in the two substances. If the incident angle is larger than the critical angle, there will be no transmitted signal and the entire signal will be reflected.

It might be desirable to get the critical angle at a certain horizon. This seismic acquisition method is called seismic refraction.

Asymptotic methods

Asymptotic methods, or "ray tracing methods", do not use the whole wave field. Instead the wavefield from the source to the receivers is treated as a series of events (raypaths).

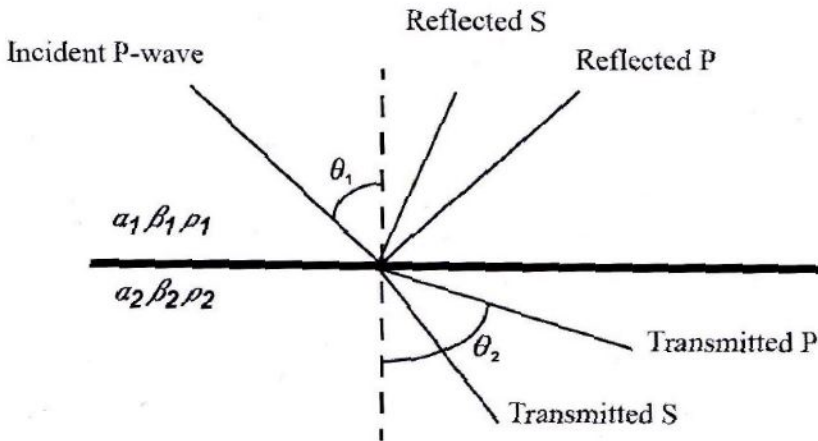


Figure 1.2: When a P-wave hits an interface between two substances, both a P-wave and an S-wave are being reflected and transmitted (Landrø, 2011).

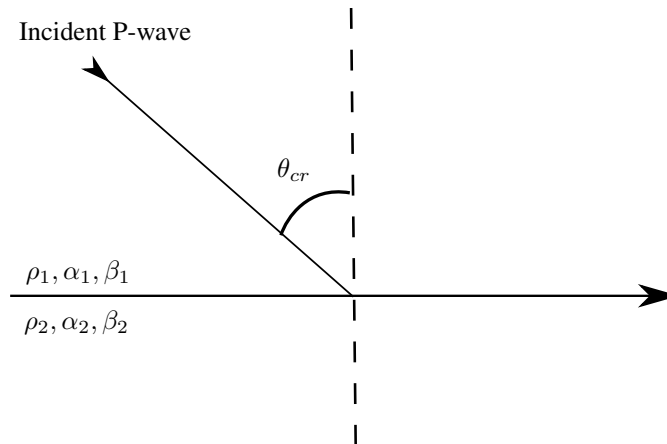


Figure 1.3: When a P-wave hits an interface between two substances at the critical angle, the refracted wave propagates along the interface.

Raypaths are calculated by either solving a differential equation derived from the seismic wave equation or by using Snell's law which apply to the a gridded model and an interface based model respectively. When using Snell's law the velocity and the direction of the raypath are constant within a heterogeneous layer. The velocity and the direction changes at an interface in accordance to the law. That means that these methods also include multiples.

The eikonal equation (1.3) is a nonlinear partial differential equation of first order. This equation describes the travel time of a seismic wave and is valid for high frequency

conditions. The eikonal equation is the basis for kinematic ray tracing, which only needs a velocity model to compute the travel times of the rays (Landrø, 2011).

$$(\nabla T)^2 = \frac{1}{v(\vec{x})^2} \quad (1.3)$$

where T is the arrival time and v is the velocity.

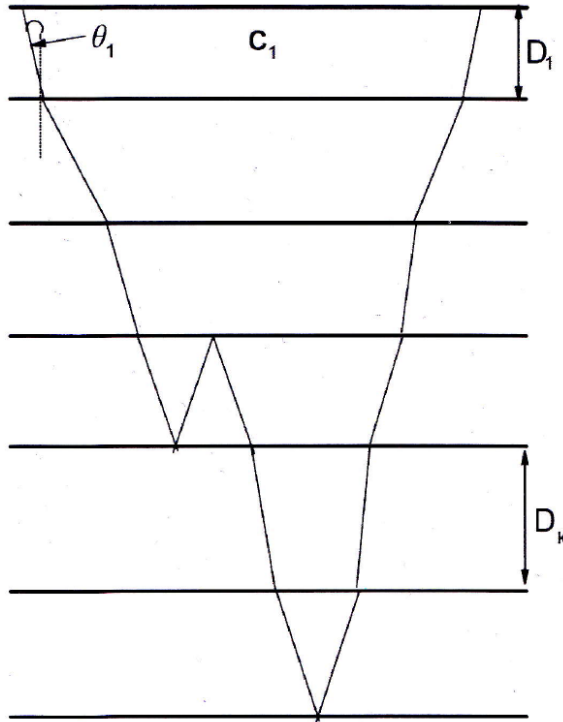


Figure 1.4: Illustration of ray tracing. At each surface the ray is transmitted or reflected in accordance to Snell's law (Landrø, 2011, p. 68).

$$2\nabla P \nabla T + P \nabla^2 T = 0 \quad (1.4)$$

where T is the arrival time and P is the Amplitude

Dynamic ray tracing, or amplitude computation, need both a velocity model and a density model. The Dynamic ray tracing is solved by using the transport equation, as given by equation (1.4), which is a linear partial differential equation of first order.

Ray tracing methods are quite accurate in the sub-critical angles and reasonably accurate for super-critical offsets but not accurate near the critical offsets (Krebs, 2004). Ray tracing can be divided into two main categories: offset and zero offset methods, depending on the source and receiver setting and the aim of the modeling.

Offset ray tracing is recorded by using the same source but different receivers. There are some different setups, for example when the source is placed at one side of the receivers. This is called off-end setup. The source can also be placed in the middle, with receivers on both sides, which is called split spread setup. Both setups simulate the acquisition of real seismic and is used to test migration algorithms and dip filtering.

Zero offset ray tracing is recorded using zero offset between the source and the receiver. Zero offset ray tracing can be used to simulate a Common Mid Point(CMP) stack section.

Because of the simplicity of this method, the computation time is short and therefore widely used to compute synthetic seismograms. Ray theory is useful for computing travel times but not always for signal amplitudes.

Direct methods

Direct methods are numerical solutions of the wave equation, hence sometimes called full wave methods. These methods need a density model and both a P-wave and an S-wave velocity model to work.

The finite difference(FD) method is one of these direct methods and it requires a grid based model to run. The FD method calculates the seismic wavefield at every grid point, by solving an approximation of the derivatives in the wave equation with finite difference formulas. Explicit finite difference methods calculate the wavefield at a given time based on the previous times. Implicit finite difference methods use both previous and future values.

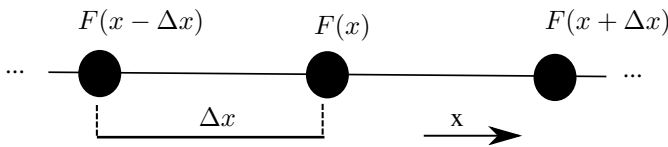


Figure 1.5: Illustration of the center-difference. The center-difference uses the surrounding grid points to calculate a center grid point.

A finite difference formula for approximating a derivative, where the function $F(x)$ has a continuous first derivative can be written as:

$$\frac{dF(x)}{dx} = \lim_{\Delta x \rightarrow 0} \frac{F(x + \Delta x) - F(x)}{\Delta x} \approx \frac{F(x) - F(x - \Delta x)}{\Delta x} \quad (1.5)$$

$$\frac{dF(x)}{dx} = \lim_{\Delta x \rightarrow 0} \frac{F(x) - F(x - \Delta x)}{\Delta x} \approx \frac{F(x) - F(x - \Delta x)}{\Delta x} \quad (1.6)$$

$$\begin{aligned} \frac{dF(x)}{dx} &= \lim_{\Delta x \rightarrow 0} \frac{F(x + \Delta x) - F(x - \Delta x)}{2\Delta x} \\ &\approx \frac{F(x + \Delta x) - F(x - \Delta x)}{2\Delta x} \end{aligned} \quad (1.7)$$

Forward-difference approximation (equation 1.5) and backward-difference approximation (equation 1.6), where Δx is the step size in the x -direction. Equation 1.7 is the center-difference approximation which is derived by adding the forward and the backward approximation.

When using approximations the solution would not be entirely correct, hence some deviation will arise. By applying the Taylor series expansion to the forward and backward approximation it can be shown that the error is of the order Δx (a linear error). For the central-difference approximation the error is in the order of $(\Delta x)^2$ (quadratic error). This shows that the central approximation is a more accurate approximation to $\frac{dF(x)}{\Delta x}$ (Krebs, 2004).

One might think that by decreasing the grid size the method would be more accurate. This is not the case. Due to the occurrence of roundoff errors, the accuracy will in fact decrease if the grid size becomes too small. It is possible to make the method more exact without changing the grid size. Then a higher-order approximation is used but this requires more computation, hence it takes more time to solve the problem.

It is also possible to have a too coarse grid. This might result in reduced accuracy and grid dispersion. As a rule of thumb the grid step should not be larger than $\frac{1}{10}$ of the size of the shortest wavelength in the wavefield (Krebs, 2004). If higher-order approximations are used, this number may be reduced. The computation time may be almost the same because the higher-order approximation is more complex.

If $F(x)$ and its derivative is known at a point x_0 , the function at $F(x + \Delta x)$ can be derived using the equation,

$$F(x + \Delta x) \approx F(x) + \frac{dF(x)}{dx} \Delta x \quad (1.8)$$

By using Taylor series to solve this equation, an approximation of the second derivative can be derived. The following equation is one of the common approximations of the second derivative.

$$\frac{d^2 F(x)}{dx^2} \approx \frac{F(x + \Delta x) - 2F(x) - F(x - \Delta x)}{\Delta x^2} \quad (1.9)$$

One of the drawbacks of the finite difference methods is that they are very time-consuming, especially for 3D models. That is why it is common to do FD calculations in 2D, because it requires less computation time. Another drawback is that the FD method generates artificial reflections which are reflections coming from the edges of the numerical grid. There are ways to reduce the strength of these reflections, like using absorption boundaries. The boundary reflections will still interfere with the reflections from the model, but the strength of the boundary reflections is less significant than the reflections from the model.

The FD method used in this thesis is a high-order approximation and will be explained in more details in Chapter 4

Problems with seismic modeling

Most of the processing algorithms require that the seismic is recorded at the same level and with a regular grid. When performing a land seismic survey, this is a challenge because of

the changing topography. The same problem is encountered in ocean bottom seismic.

Complexities like faulting and folding and high velocity layers near the surface causes an illumination problem for deeper targets. These structures cause scattering, which complicates the wave propagation. Also source generated noise may be trapped in the near surface and interfere with the recorded signal (Alaei, 2012).

There are several complex structures in the subsurface that also complicate the wave propagation and the seismic modeling:

1. Salt usually has a high velocity compared to the surrounding sediments. The signal to noise ratio is usually low in the proximity of the salt, especially beneath the salt.
2. Formations exposed to folding and thrusting usually have a complex internal structure with highly dipping layers. This results in some parts with good and some parts with poor illumination in the subsurface.
3. Fault usually cause a fault shadow which is an area with poor illumination beneath the fault. This cause the seismic to be unreliable in this zone.
4. Lateral lithology variations may be caused by simple structures, but the velocity variations in such structures may cause complex seismic waves.

Model Building

2.1 Background Material

The outcrop section which this work is based on is the outcrop of Storvola alongside Van Keulenfjorden on southern Svalbard in the Norwegian Arctic.

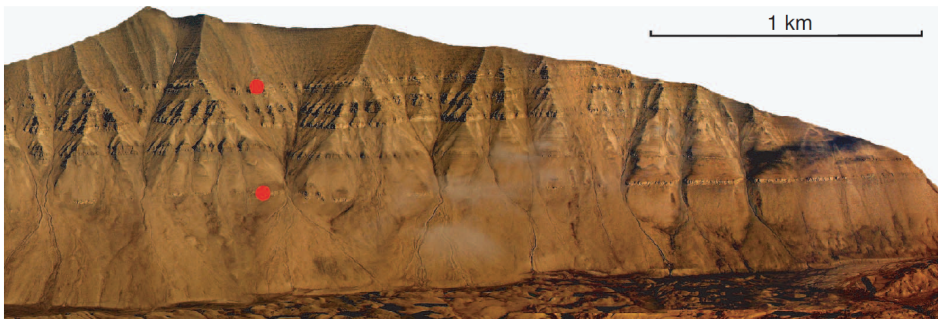


Figure 2.1: Picture of the outcrop of Storvola, located alongside Van Keulenfjorden on southern Svalbard in the Norwegian Arctic (Johansen et al., 2007)

Before beginning the modeling of the outcrop, the dimension of the outcrop needs to be decided. The length of the model is 10km and the depth is 800m . The model should be buried beneath a 1000m layer of seawater, to avoid seabed multiples and to simulate an offshore section. The total depth of the model should be 1800m . The model was planned to be a so called 2,5-D model, that is a 3-D model that has constant values in its third dimension.

Johansen et al. (2007) performed an outcrop study where they mapped the geology of this outcrop and the surroundings. The result of the geological study is shown in Figure 2.2. As seen, they also made an interpretation of the geology in between the outcrops.

At the same time the physical properties of the P-and S-wave velocities and densities

were measured, by acquiring rock samples and performing laboratory measurements. The resulting model from the measured P-velocity can be seen in Figure 2.3. One such model was generated for each property; the geometry is the same but the values it contains is different. In this work, these properties are used to build the property models. As mentioned in the the introduction, a normal way to assign properties is to keep the values constant inside a layer, which also applies to this work. This is done because the parameters vary in every dimension and only a few samples were taken from each layer, hence the values assigned are the average value and must be considered an approximation (Johansen et al., 2007).

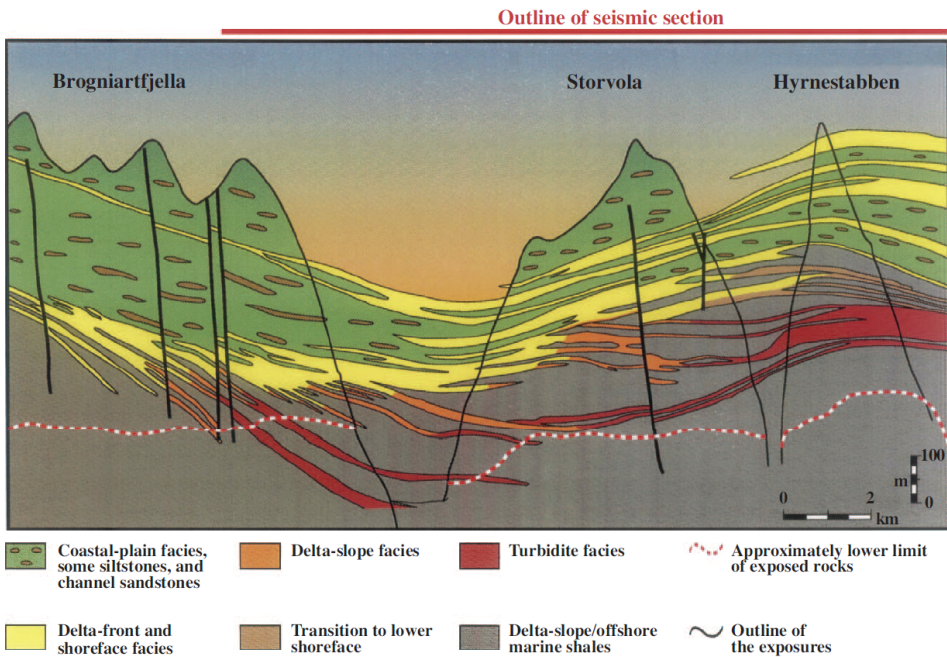


Figure 2.2: Geological model of Storvola and the surroundings with interpreted geology in between the outcrops (Johansen et al., 2007).

On figure 2.3 the top coastal plain deposits above the yellow sandstones in figure 2.2 have been removed. Both figure 2.2 and 2.3 are illustrations of the geological model and show a simple geometry. Since the geometry is easy to generate, every detail from the picture should be modelled to get a more accurate geophysical model. The forward seismic realization algorithm used in this work needs a grid based model.

2.2 Building a model in Petrel

When building a model in Petrel out of a picture, like figure 2.2, it is possible to draw lines (called polygons in Petrel) on the picture (SCM, 2011).

When drawing a set of selected points along a horizon on the picture (see figure 2.4),

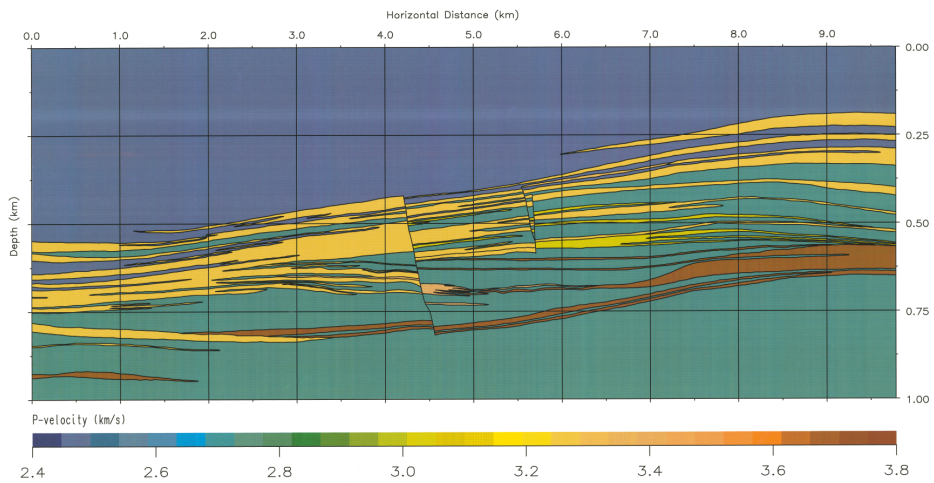


Figure 2.3: P-velocity model of Storvola, the top coastal plain deposits above the yellow sandstone have been removed (Johansen et al., 2007).

Petrel automatically uses linear interpolation between the picked points and the boundary. The next step is to convert these drawn lines into surfaces.

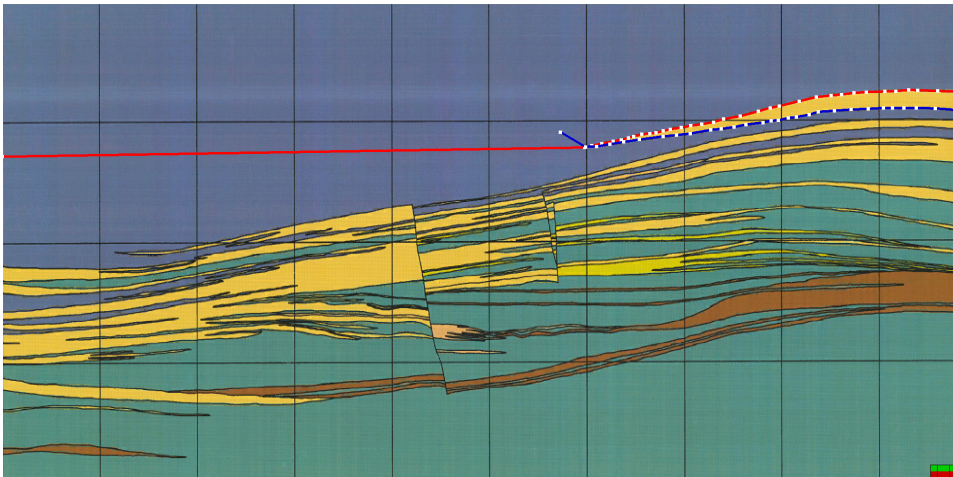


Figure 2.4: Picked horizons on a picture in Petrel. The software automatically interpolate between the picked points and the boundary.

When converting the drawn lines into surfaces the, size of the surface and the algorithm which converts the drawn line to a surface need to be decided. In this work the algorithm *closest* is used. This algorithm tries to keep the surface as close to the drawn line as possible, but the algorithm follows the structured grid of the model, which implies a lot of sharp edges. The way to remove these edges is a smoothing operation. Be advised that

the smoothing parameters may cause the surfaces to move off the horizons, so be careful when choosing parameters and always do a quality control of the results after smoothing. Some times it is necessary to generate the surface again and change some parameters to get a better match between the surface and the boundary on the picture.

It is also possible to move surfaces, this was done to flatten the model to simulate a newly deposited delta. To move all the surfaces according to the flattening, a difference surface was generated, which is a mathematical surface, not a geological surface. This difference surface varies in depth according to the difference in the depth between the flattening surface and the horizontal surface. The flattening surface is the surface assumed to be the top layer at the time of deposition of the top layer in the model and the horizontal surface is the surface assumed to be the correct position at the time of deposition. The difference surface could now be added to every surface, which would move all the surfaces (see figure 2.5).

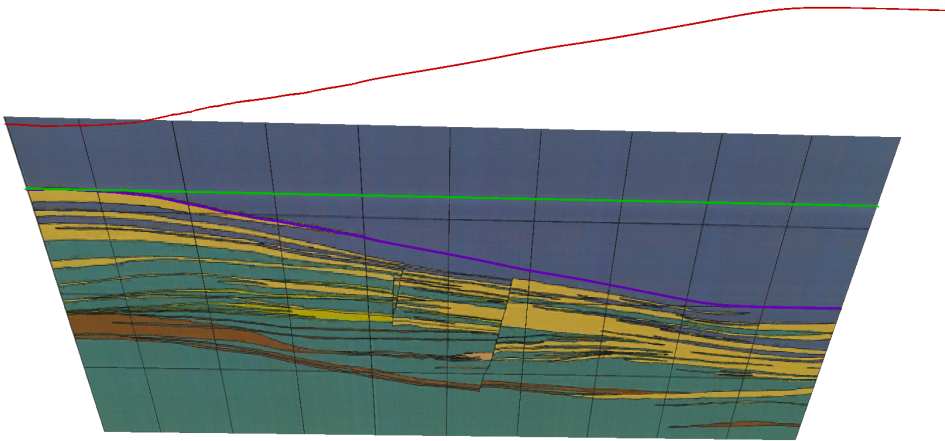


Figure 2.5: The purple surface is the surface called the flattening surface. The green surface is the horizontal surface, which intersects the flattening surface at its minimum point. The flattening surface should look like the green surface after its flatten. The red surface is the difference surface, which is the difference between the purple and the green surface.

After all the surfaces have been generated, it is time to build the property model. First a structured grid needs to be generated where the spacing between the grid points are decided. This volume of grid points is the basis for the property model.

The model is now ready to get assigned values. The way this is done is to use two surfaces, one top and one base, and assign a value between these surfaces. The surfaces need to cross the model, but not all layers fulfills this criteria. To solve this problem the surfaces are set to be equal everywhere except in the area of the layer, hence no values are assigned other than those in the area of the layer. It is also possible to assign a value outside the area between the two surfaces. This is generally not used, except when assigning values for the first time. It is a good idea to assign a value outside the area between the surfaces that covers much of the area in the model and is hard to map, like for instance the dark green color in figure 2.3. This is handy because it is easy to overwrite this value later

by "real" values. It also assures that all the grid points are assigned a value, in case the surfaces do not manage to fill them all, which would give problems in the seismic modeling part.

Lithology/facies	P-velocity ($\frac{m}{s}$)	S-velocity ($\frac{m}{s}$)	Density ($\frac{Kg}{m^3}$)
Turbidite facies	3650	2500	2600
Marine shales	2750	1900	2500
Delta slope	3400	2250	2600
Top shale	2300-2500	600-800	2300
Delta Front	3300	2300	2600
Transition to lower shoreface	3050	2170	2600
Seawater	1500	0	1000

Table 2.1: The geophysical values of P-wave velocity, S-wave velocity and densities used in building the property models. The values are adapted from Johansen et al. (2007).

After all properties have been inserted into the model, the result for the p-velocity looks like figure 2.6. For figure 2.6 the surfaces have also been buried beneath 1000m of seawater and a 200m layer of shale as an overburden. This model, together with a density and an S-velocity model with similar geometry, have been made and are used as an input in seismic forward modeling (see Appendix A figure A.2 and A.3).

More about how to generate property models and the use of Petrel to do this can be found in Appendix B.

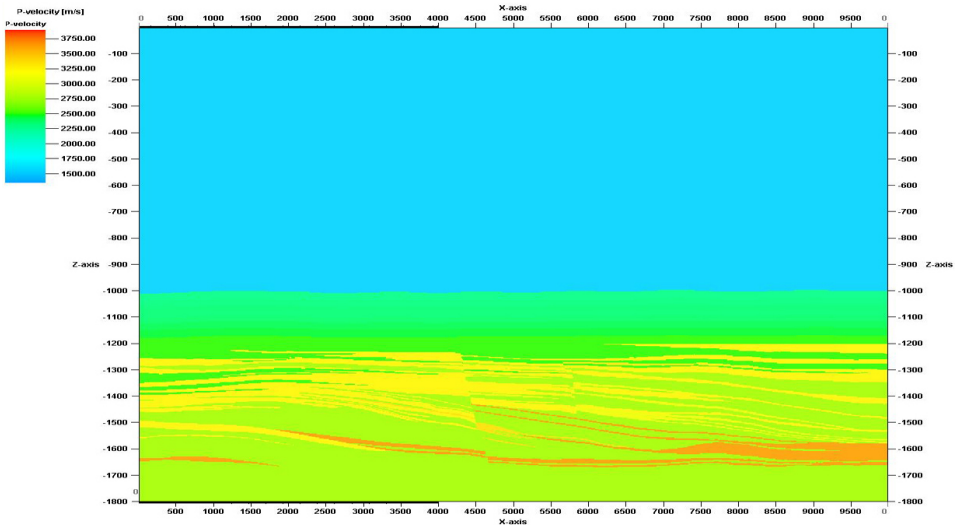


Figure 2.6: P-velocity model built in Petrel. The property model from Johansen et al. (2007) (figure 2.3) has been flattened at the top right yellow sandstone, and buried beneath 1000m of seawater and 200m of shale. This model can be used as an input in seismic forward modeling together with a similar density and V_s -property model. For a larger picture see Appendix A figure A.1.

Converting

3.1 Convert the geological model from Petrel to Madagascar

Madagascar is an open-source software for multidimensional data analysis and reproducible computational experiments. Madagascar uses a simple file format called Regularly Sampled Format (RSF). This file consists of a header part and a binary part, often separated into two files. The header file is an ASCII text file (readable for humans) with suffix .rsf and is usually stored locally. The binary part is usually stored in a separate directory with the suffix .rsf@. It is this binary file that contains the data.

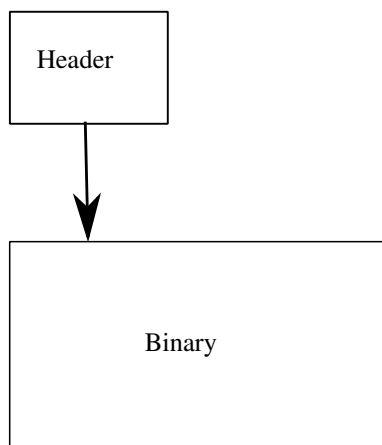


Figure 3.1: Illustration of the RSF file format. The header file points to the binary file, which contains the data. The header file contains the attributes of the RSF that can be read by humans (from Madagascar (2013)).

The property models built in Petrel can not be exported to RSF file format directly. That is why a program exists to convert ECLIPSE files to the RSF file format (the step to do this is explained in Appendix C). ECLIPSE is mainly a reservoir simulation tool developed by Schlumberger, which also sells the Petrel software. Schlumberger (2013) describe ECLIPSE like this: "ECLIPSE is a numerical solution for fast and accurate prediction of dynamic behavior for all types of reservoirs and degree of complexity, structure, geology, fluids and development schemes."

Because the ECLIPSE software and Petrel are owned by the same company, it is possible to export Petrel models into ECLIPSE format and do simulations on the models. In this work the ECLIPSE format is just the first stop when converting the models. A program in the Madagascar software called *sfpetread* uses the ECLIPSE files as input and converts them into RSF files. The P-velocity model displayed in figure 3.2 is the converted model which is readable for Madagascar. The corresponding models for the S-velocity and density can be found in Appendix A figure A.5 and A.6

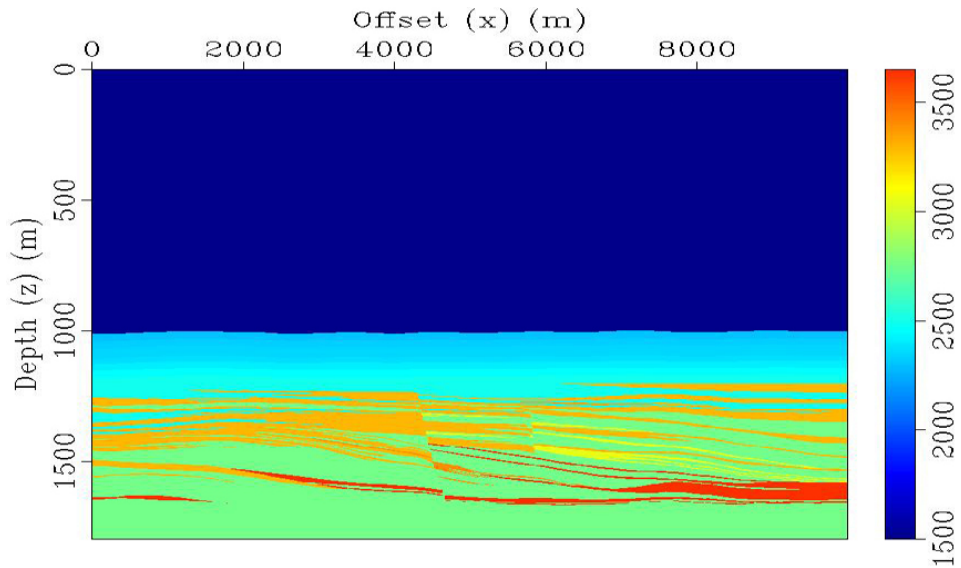


Figure 3.2: Converted P-velocity model from Petrel through ECLIPSE to Madagascar. A large scale figure can be found in Appendix A figure A.4.

Seismic Modeling

4.1 Madagascar software

A decision to reduce the property models to 2D was made to ease the computation time. Then the Madagascar software only needs to solve the 2D elastic wave equation using a 2D finite difference method. The method predicts the seismic wavefield and the responses of the subsurface model.

In the 2D coordinate system the horizontal axis is x and the vertical axis is z . Virieux (1989) solves the elastodynamic equations instead of the acoustic wave equation. The medium is assumed to be linearly elastic and isotropic, which for a 2D situation are:

$$\begin{aligned}
 \frac{\partial^2 u_x}{\partial t^2} &= \frac{1}{\rho} \left(\frac{\partial \tau_{xx}}{\partial x} + \frac{\partial \tau_{xz}}{\partial z} \right), \\
 \frac{\partial^2 u_z}{\partial t^2} &= \frac{1}{\rho} \left(\frac{\partial \tau_{xz}}{\partial x} + \frac{\partial \tau_{zz}}{\partial z} \right), \\
 \tau_{xx} &= (\lambda + 2\mu) \frac{\partial u_x}{\partial x} + \lambda \frac{\partial u_z}{\partial z}, \\
 \tau_{zz} &= (\lambda + 2\mu) \frac{\partial u_z}{\partial z} + \lambda \frac{\partial u_x}{\partial x}, \\
 \tau_{xz} &= \mu \left(\frac{\partial u_x}{\partial z} + \frac{\partial u_z}{\partial x} \right)
 \end{aligned} \tag{4.1}$$

where u_x and u_z are displacement vectors, τ_{xx} , τ_{zz} and τ_{xz} is stress tensors, ρ is the density, and λ and μ are the Lamè coefficients.

The equations in equation 4.1 can be transformed into first-order hyperbolic equations

$$\begin{aligned}
\frac{\partial v_x}{\partial t} &= \frac{1}{\rho} \left(\frac{\partial \tau_{xx}}{\partial x} + \frac{\partial \tau_{xz}}{\partial z} \right), \\
\frac{\partial v_z}{\partial t} &= \frac{1}{\rho} \left(\frac{\partial \tau_{xz}}{\partial x} + \frac{\partial \tau_{zz}}{\partial z} \right), \\
\frac{\partial \tau_{xx}}{\partial t} &= (\lambda + 2\mu) \frac{\partial v_x}{\partial x} + \lambda \frac{\partial v_z}{\partial z}, \\
\frac{\partial \tau_{zz}}{\partial t} &= (\lambda + 2\mu) \frac{\partial v_z}{\partial z} + \lambda \frac{\partial v_x}{\partial x}, \\
\frac{\partial \tau_{xz}}{\partial t} &= \mu \left(\frac{\partial v_x}{\partial z} + \frac{\partial v_z}{\partial x} \right)
\end{aligned} \tag{4.2}$$

where v_x and v_z are velocity vectors.

At the time $t = 0$ everything is set to be in equilibrium and the stress and velocity are set to zero everywhere in the the medium. For the four edges of the model Perfectly Matched Layer (PML) is added. The PML reduces the signal that hits the boundaries so that the reflected signals from the boundaries are weak and ideally do not interfere with the reflections from inside the medium. At the surface a stress-free condition, or a free-surface condition is used. This free surface do not reflect any signal, hence no seabed multiple or ghost reflections in the dataset. Because of this it was possible to cut 750 meter of seawater from the top of figure 3.2 resulting in figure 4.1. The removal of this data saved a lot of computation time.

The last parameter to set is the source signal. For this software a Ricker wavelet is used. The specter of the Ricker wavelet needs to fulfill the Nyquist criteria, which is

$$f_{max} \leq \frac{C_{min}}{2\Delta x} \tag{4.3}$$

where f_{max} is the max frequency in the wavelet specter, C_{min} is the minimum velocity in the models (considering both the P- and S-wave velocities, most likely it will be an S-wave velocity), Δx is the distance between two grid points in meters.

Another criteria that needs to be fulfilled is the Nyquist sampling theorem.

$$\Delta t \leq \frac{\sqrt{2}}{\pi} \frac{\Delta x}{C_{max}} \tag{4.4}$$

where Δt is the sampling interval in time and C_{max} is the maximum velocity in the models (considering both the S and P-wave velocities).

When the signal go off the stresses in the medium change and the wave starts to propagate through the medium at the given velocity in the layers.

The final step is to discretise the derivatives in equation 4.2 into a central finite difference, as given by the example equation 1.7, but now in 2D and for even more grid points. These equations, found by Virieux (1989), are used to predict the wavefield for a user defined time and record the signals that hit the receivers.

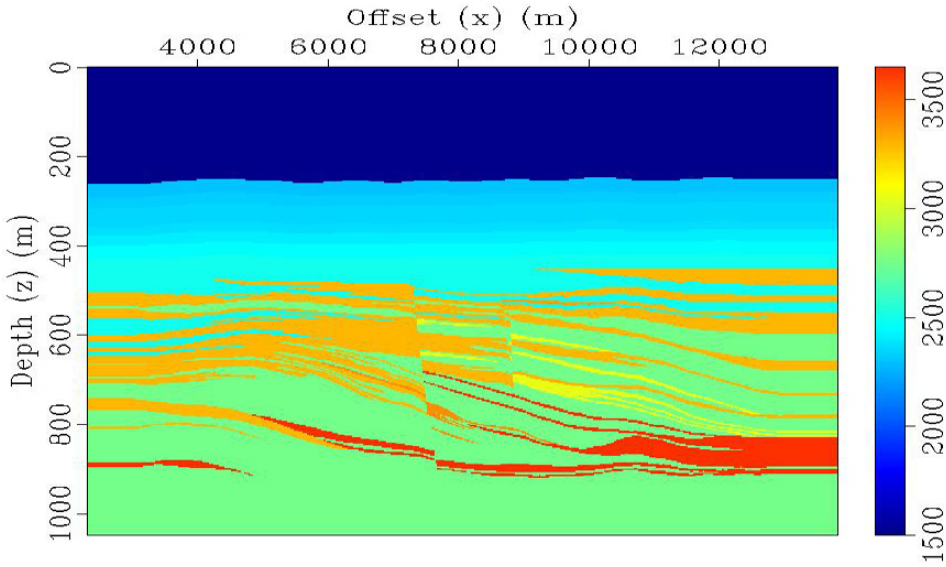


Figure 4.1: The same figure as figure 3.2 but this has been cut. The top 750 meters has been removed because of the free surface parameter in the software. The model has also been extended on both sides, this to get full fold over the entire area of interest when acquire the seismic. A large scale figure can be found in Appendix A figure A.7.

4.2 Stability

For the FD method to be stable the equations 4.3 and 4.4 need to be fulfilled. For the Nyquist criteria in equation 4.3 the model has a $\Delta x = 3$ meters and $C_{min} = 600 \frac{m}{s}$. This gives a frequency of

$$f_{max} \leq \frac{C_{min}}{2\Delta x} \leq \frac{600}{2 \times 3} \leq 100 \text{ Hz} \quad (4.5)$$

The maximum frequency in the wavelet specter needs to be less or equal to 100Hz. The Ricker wavelet used and the specter can be seen in 4.2

The Nyquist sampling theorem, given by equation 4.4, is used to calculate the highest time sampling interval where the equations are still stable. The model has a $C_{max} = 3650 \frac{m}{s}$ as its highest velocity. The maximum sampling interval becomes:

$$\Delta t \leq \frac{\sqrt{2}}{\pi} \frac{\Delta x}{C_{max}} \leq \frac{\sqrt{2}}{\pi} \frac{3}{3650} \lesssim 0.369 \text{ ms} \quad (4.6)$$

If these two equations are fulfilled the FD equations should be stable and give correct results.

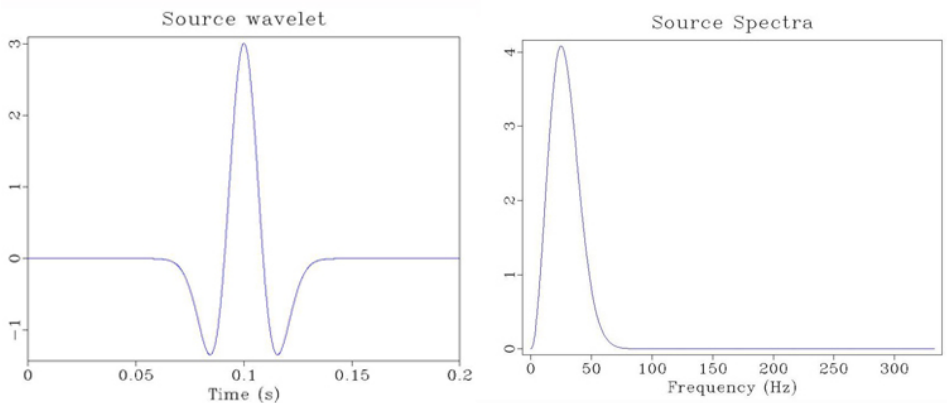


Figure 4.2: The figure to the left is the Ricker wavelet used in the calculation and the figure to the right is the specter of the wavelet. As can be seen, the frequency content is within the Nyquist frequency of 100 Hz.

4.3 Seismic Modeling

The seismic modeling simulates a seismic survey by solving the finite difference equations derived from equation 4.2. The FD methods make a prediction of the seismic wave field based on the property models. Figure 4.3 shows two wave predictions from the same shot at the times 0.5 sec and 0.84 sec. In the figure at 0.5 sec the wave has not yet hit any boundary and has not been reflected. 0.34 sec later a clear wave is propagating towards the surface.

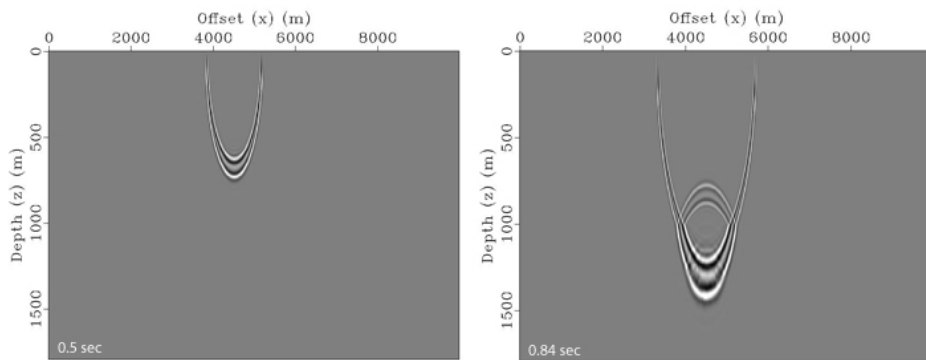


Figure 4.3: The two figures are from the same shot but at different times. The figure to the left is from 0.5 seconds after the source fired. The predicted wave field has not yet hit any boundaries. The figure to the right is from 0.84 seconds after the source fired and a reflecting wave is clearly visible.

To perform a seismic acquisition survey several parameters need to be set, like the source depth and cable settings. These parameters are used to set up the geometry of

the receiver array, but also constants like the total sampling time and time between the samples. The parameters used in this study are listed in table 4.1 and the setup is shown in figure 4.4.

To solve the fine difference equations an enormous amount of computation power are required, that is why a supercomputer do all the computations. A supercomputer is basically a cluster of computers, which is connected and work together so it can be viewed as a single system. Because every shot is independent, several shots may be predicted at the same time. The required computation time depends on the amount of processors used, numbers of shots and computation time per shot.

$$T_{total} = \frac{N}{P}t_s \quad (4.7)$$

where T_{total} is the total required time, N are the numbers of shots, P are the number of processors and t_s are the time per shot, assuming equal time per shot.

Acquisition Parameters	
Parameter	Value
Source depth	9 m
Shot interval	12 m
Maximum frequency content	100 Hz
Cable depth	9 m
Cable length	1140 m
Receiver spacing	6 m
Sampling time	1.5 s
Time step	0.1 ms
Number of shots	864

Table 4.1: The acquisition parameters used in the seismic acquisition modeling.

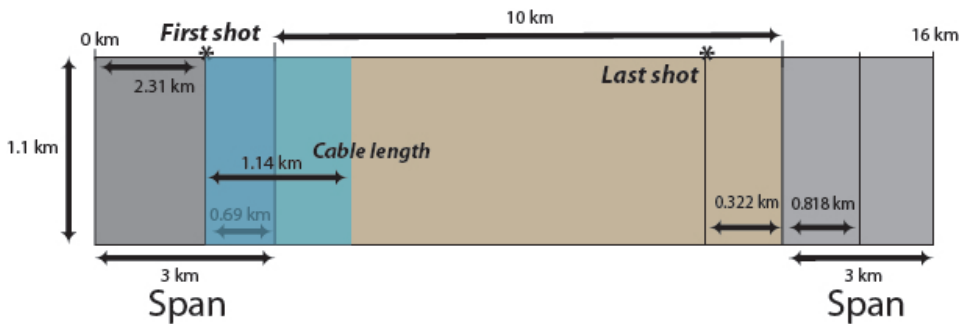


Figure 4.4: The source and receiver positions used in the seismic acquisition modeling.

The results from the seismic modeling are the recordings from the receivers displayed in a common shot gather. All the common shot gathers generated by the software are raw data. By itself, these shot gathers does not tell much about the subsurface, but when they

are put together they generate a picture of the subsurface. To accomplish this, the data needs to be processed.

Seismic Processing and Interpretation

One of the common shot gathers from the seismic modeling can be seen in figure 5.1. The direct wave is easily seen together with the sea floor reflector, and many other reflections are visible beneath the sea floor reflection. These reflections are reflections from the layers in the model and probably some internal multiples.

5.1 Processing

The process used on the seismic data is a simple processing flow and it gives a usable result. The first step is to resample the seismic data. The next step is to remove/mute the direct arrival before the muted data is sorted into CMPs. A velocity analysis is performed to generate a velocity model to be used in the migration. The last step in the processing is to perform the migration with the interval velocity model and the CMPs as input.

5.1.1 Re-sample

It is shown by Arntsen (2011) that the maximum re-sampled sampling interval can be written as:

$$f_{Nyq} \leq \frac{1}{2\Delta t} \tag{5.1}$$

where, in this case, the $f_{Nyq} = f_{max} = 100$ Hz which is the maximum frequency content in the dataset. Then Δt in equation 5.1 becomes 5 ms, which is the highest sampling interval possible before the data becomes aliased. This means that it is safe to use a new time sampling interval of 5 ms or less. In this work the data is re-sampled to 4 ms, which gives a small margin of safety. The re-sampling reduces the amount of data to be processed, hence speeds up the processing without losing data quality.

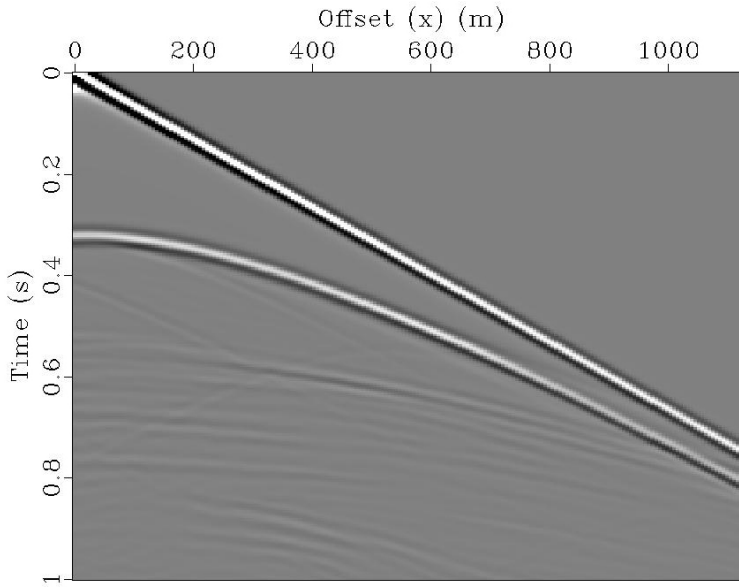


Figure 5.1: A common shot gather from the seismic modeling. For every shot fired in the survey a common shot gather like this is generated. The direct wave is easily seen together with the sea floor reflector.

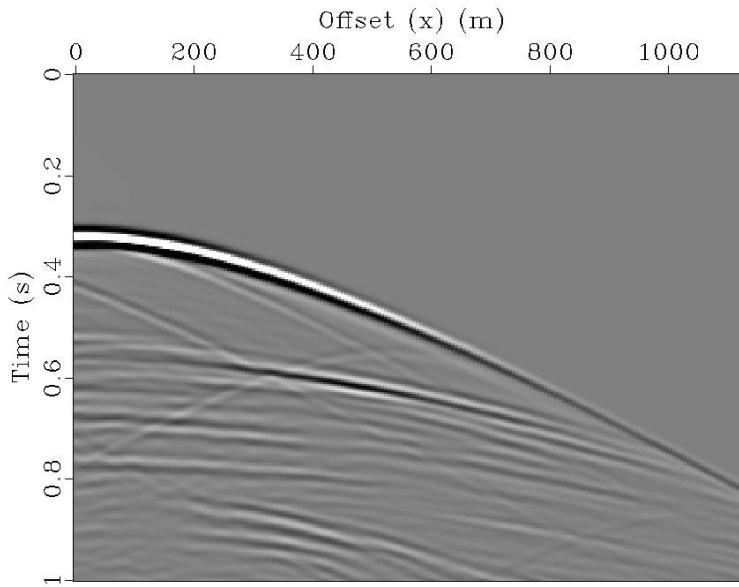


Figure 5.2: The result after applying the mute on the data in figure 5.1. The direct wave has now been removed from the dataset.

5.1.2 Mute

In this step it is desirable to mute and remove unwanted signals and, mainly, the direct wave. The direct wave is the wave that travels directly from the source to the receiver in the water layer. To do this, a filter is applied to the area where the direct wave signal is. This filter removes the signal in the area and attenuate the signal close to the filter border. This attenuation is done to avoid Gibbs phenomenon (Arntsen, 2011), which is solved by having a smooth transition of the signal strength close to the border. The result can be seen in figure 5.2, which is the same shot gather as in figure 5.1. It is easy to see that the direct wave has been completely removed and the signal strength close to the direct wave has been attenuated.

5.1.3 Sort into Common Midpoint - gather

The seismic shot data is now sorted into Common Midpoints (CMPs). A CMP is a point on the surface halfway between the source and the receivers, which is shared by several source-receiver pairs. The advantage of using midpoints is that they roughly represent the same location, which simplifies the generation of pictures of the subsurface (Landrø, 2008). Figure 5.4 shows the geometry of a CMP-gather.

A CMP-gather is generated by combining all source-receiver pairs that have the same midpoint. When displaying a CMP-gather, the traces within the gather are displayed in correspondence to the offset (see figure 5.3).

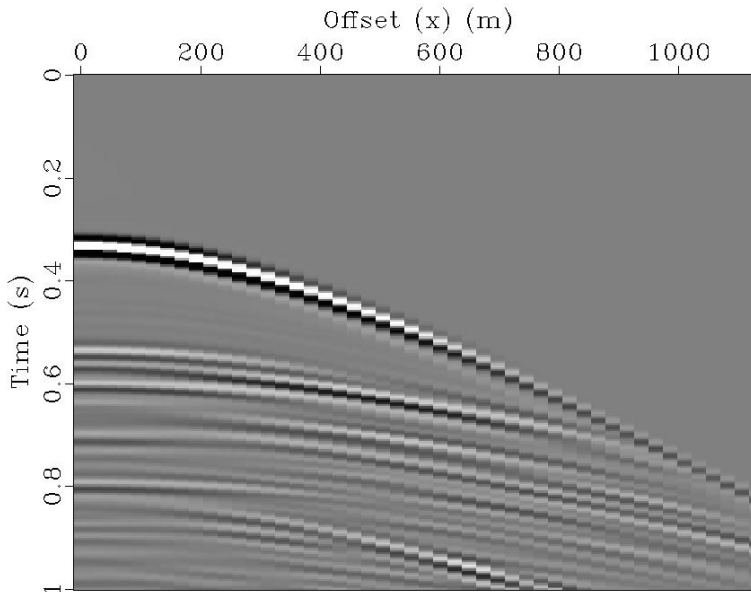


Figure 5.3: One of the common midpoint gathers from the dataset. The horizontal shifts in the data is due to the fact that a CMP only contain 48 traces.

The number of CMPs in a dataset is given by the equation:

$$M = \frac{R\Delta r}{2\Delta s} \quad (5.2)$$

where M is the number of traces per CMP, also called the fold, R is the number of receivers, Δr is the receiver spacing and Δs is the shot interval. If the values from table 4.1 are inserted, the maximum fold becomes:

$$M = \frac{\frac{1140}{6} \cdot 6}{2 \cdot 12} = 47,5 \approx 48 \quad (5.3)$$

The spacing between each CMP is half the receiver spacing, which become 3 m. The number of CMPs are given by the following equation:

$$N_{cmp} = N_s \cdot \frac{\Delta s}{\frac{\Delta r}{2}} + R - 1 \quad (5.4)$$

where N_{cmp} is the number of CMPs in the dataset, N_s is the number of shots, Δs is the shot interval, Δr is the receiver spacing and R is the number of receivers. If the values from table 4.1 are inserted, the number of CMPs in the dataset becomes:

$$N_{cmp} = 864 \cdot \frac{12}{\frac{6}{2}} + \frac{1140}{6} - 1 = 3645 \quad (5.5)$$

Ideally should figure 5.3 look as smooth as figure 5.2. The reason for the poor resolution in figure 5.2 is due to less data content than figure 5.3. Figure 5.3 displays one CMP with 48 traces and figure 5.2 displays one shot with 190 traces. Another explanation could be aliasing caused by the visualization software, but this is less likely.

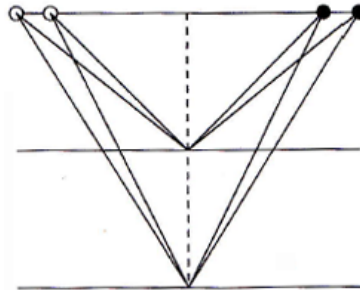


Figure 5.4: Geometry of a common midpoint gather (Arntsen, 2011).

5.1.4 Velocity Analysis

The migration algorithm needs a velocity model. In a real seismic process, a velocity picking would be performed at this stage. For every CMP, a semblance plot can be generated. "The semblance plot is a hyperbolic Radon transform, in which the amplitudes are smoothed, scaled, and contoured to produce a visual display. This transformed display has axis of time and velocity that are used to identify the velocities for normal moveout (NMO)

correction of the CMP gathers. The hyperbolic moveout energy from primary reflections, multiples, and mode converted energy is focused to a small local area on the semblance plot, with its peak defining the moveout velocity” (Bancroft and Cao, 2004). By picking the peak values in the semblance plot, and interpolate between the picked points a velocity model can be estimated. The peaks in the semblance plot are the velocities with the highest probability to be the correct velocity at that travel time (Landrø, 2008).

In this study the same P-velocity model used in the seismic modeling is used to process the data. The velocity model has been smoothed by converting the original model (4.1) into a rms-velocity model see figure 5.5.

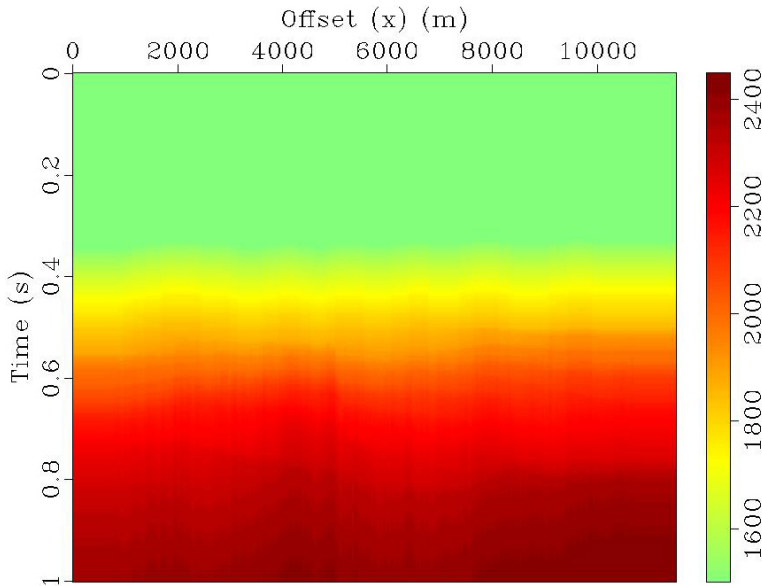


Figure 5.5: The rms-velocity model generated from the P-wave velocity model in figure 4.1.

5.1.5 Migration

Migration is the process which re-locates seismic events from the recorded location to the location where the event occurred in the subsurface. The migration creates a more accurate image of the subsurface (Landrø, 2008).

The migration algorithm used in this study is a 2-D Prestack Kirchhoff time migration with anti-aliasing. The Kirchhoff migration is one of the simplest migration algorithms that exists and it needs only a RMS velocity model to work.

For diffraction hyperbolas in a source-receiver pair, which in this case is from the CMP-gathers, the hyperbola has its origin at a point in the subsurface. It is possible to split the travel time into a downgoing travel time and an upgoing travel time. The downgoing wave emits from the source and the upgoing from the receivers. At the point of diffraction, they meet. The total travel time is the summation of the downgoing and the upgoing wave.

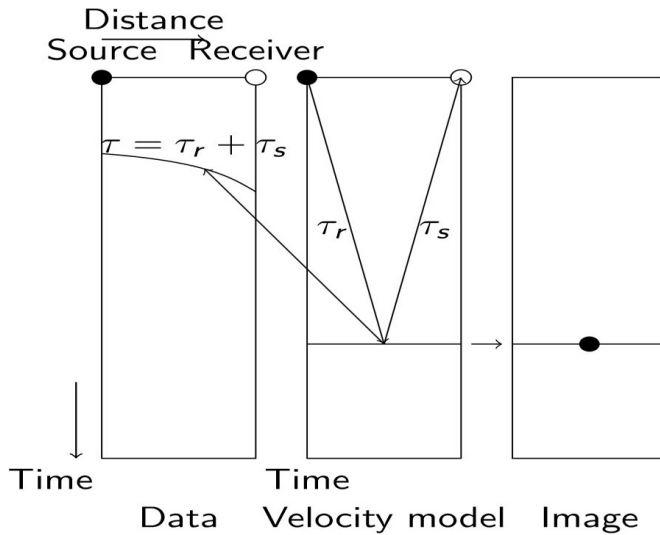


Figure 5.6: Kirchhoff time migration illustration adapted from (Arntsen, 2012). First the travel times are calculated and correlated to the data. If there exist a diffraction hyperbola, the reflection point in the velocity model correspond to the same point on the migrated image.

When trying many different possibilities and combinations of raypaths (straight lines) in the velocity models, it is possible to compute these travel times, using equation 5.6.

$$\begin{aligned} \tau_s &= \sqrt{\frac{(x - x_s)^2 + (y - y_s)^2}{c^2} + \tau_0^2} \\ \tau_r &= \sqrt{\frac{(x - x_r)^2 + (y - y_r)^2}{c^2} + \tau_0^2} \end{aligned} \tag{5.6}$$

were (x_r, y_r) and (x_s, y_s) are the receiver and source positions respectively, while $\tau_0 = \frac{z}{c(z)}$ is equal to the vertical traveltimes and the velocity $c = c(z)$ is only depth dependent.

After computing the total travel time. The migration algorithm run a check in the seismic data at that time, to see if a hyperbola exist. If there exist a hyperbola at that time. The reflection point in the velocity model correspond to the same point on the migrated image. (Arntsen, 2012). The result after migration is shown in figure 5.7

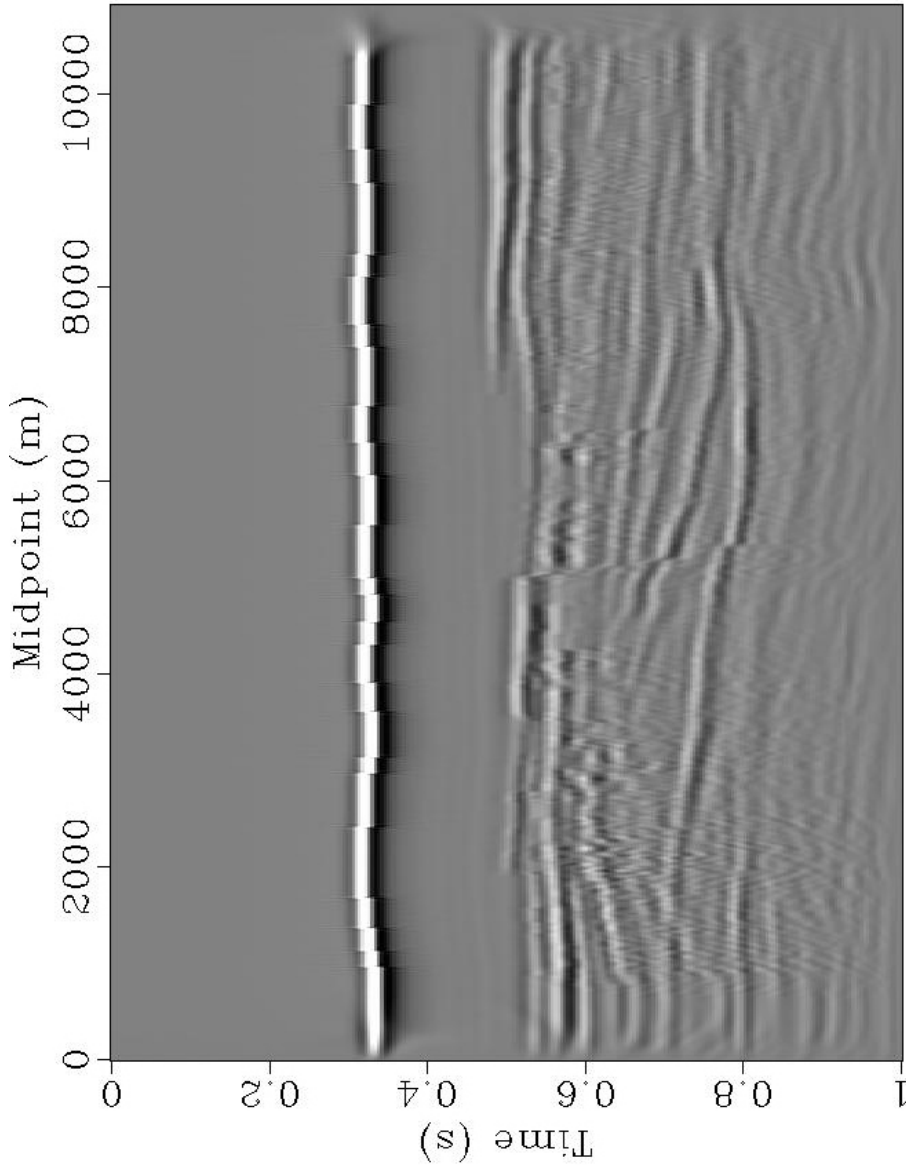


Figure 5.7: The migrated data, after performing the 2-D prestack Kirchhoff time migration algorithm.

5.2 Interpretation of the Synthetic Seismic

In order to compare the synthetic seismic to the geological model, the synthetic seismic in figure 5.7 needs to be interpreted. The interpretation was performed by following the visible reflections and without looking at the geological model. This was done to ensure that the interpretation decisions were not influenced by the geological model. Horizons and faults that were present in the geological model but were not visible on the synthetic seismic were not interpreted.

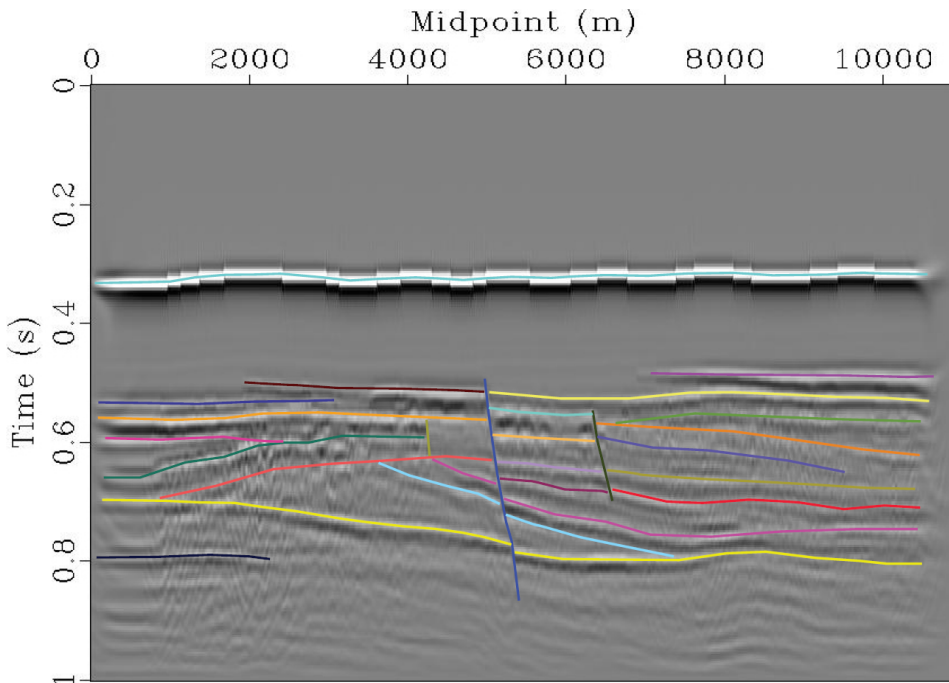


Figure 5.8: Interpretation of the synthetic seismic using a greyscale color mapping. See appendix A figure A.8 for a larger picture.

The interpretation was performed on the positive reflection values, which in greyscale are the white areas. The colors of the interpreted horizons and faults are chosen to avoid similar colors and misunderstandings. The only exceptions are horizons interpreted as the same layer cross faults, then the same color is used on both horizons.

On figure 5.8 a greyscale color mapping is used, on figure 5.9 a read-white-blue color mapping is used. On different color mappings, different details can be visible. The layering on the right hand side in figure 5.9 are clearer than the corresponding layers in figure 5.8. By looking at and combining different color mappings, it is possible to interpret the data with more accuracy and certainty.

Three faults were interpreted in figure 5.7. The middle and right fault are the most noticeable, because is is a clear shift in the reflections. The left fault is at the end of an area containing a bit obscure data, and it is worth noticing that there are no clear reflections

in the vicinity on the right side of the fault.

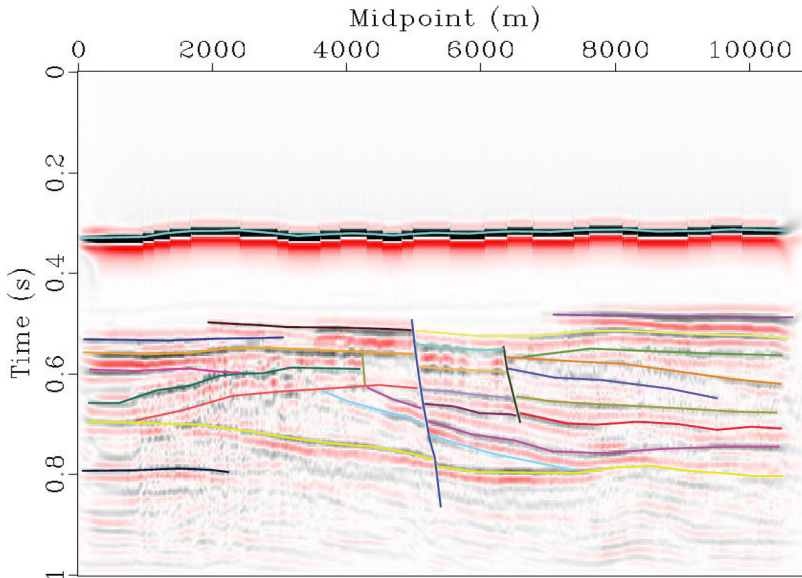


Figure 5.9: Interpretation of the synthetic seismic using a red-white-blue color mapping. See appendix A figure A.9 for a larger picture.

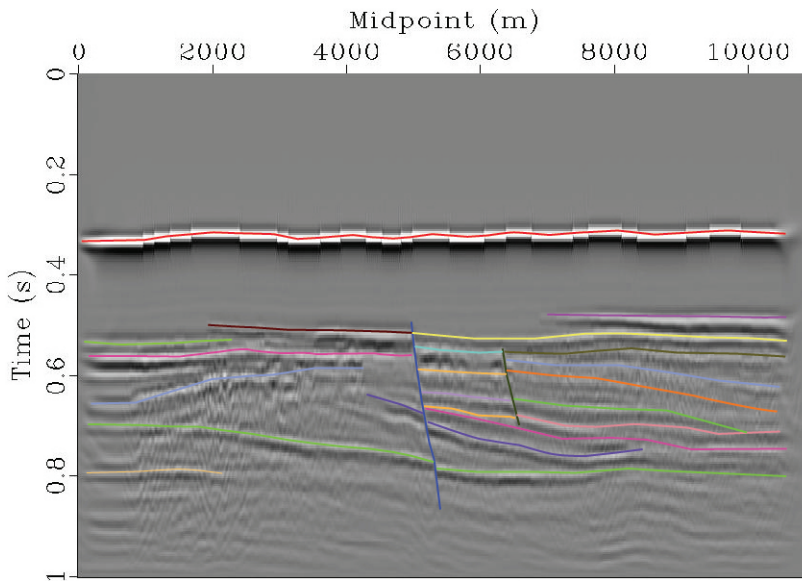


Figure 5.10: Interpretation of the visible layers in the geological model on the synthetic seismic. See appendix A figure A.10 for a larger picture.

To the right of the middle fault the data is of good quality and the reflections are clear and continuous. On the left hand side the data is a bit blurred and the reflections in this area are not as continuous as the ones to the right. This made it harder to interpret the seismic.

The interpretation of figure 5.10 was done by comparing the seismic line and the geological model, to see if it was possible to do other decisions when interpreted figure 5.8. On the left side of figure 5.10, where the data is noisy, it was too much interference to be certain of any layering, therefore very few interpreted layers.

Discussion

6.1 Model Building

The first step in this project was to digitize a picture of a P-wave velocity model representing a geological model (figure 2.3). There was no fast way to digitize the model, but Petrel has some processes that can do the digitalization (SCM, 2011). By digitizing one layer at the time and converting them into surfaces, the property models grow at a steady pace. The digitalization of the layers were not a complicated process but it was a time consuming process.

The fattening operation was performed so that the model should look like a newly deposited delta. This was a bit challenging, because no processes exists in Petrel that flattens a surface directly, and were the other layers are effected by the flattening. That is why a mathematical surface was added to all the surfaces. By doing this, the flattening was done manually. A automatic flattening process would most likely do the same operation, but faster.

Looking at the result after the flattening operation, it is a possibility that at one time in the past, this section looked like figure 2.6. The flattening operation tries to reverse some of the deformation the formation has undergone.

6.2 Generation of the Synthetic Seismic

When beginning the seismic modeling, several single shots were performed to find the correct acquisition parameters for the survey. The single shot result could tell if the data was aliased, a correction to the source wavelet might solve that problem. The most important test performed in the single shots was to ensure the stability of the seismic realization algorithm. After the single shot modeling it was time for a large scale acquisition on the supercomputer. Several small scale surveys were executed to set the final parameters. The receiver and source position was some of the new parameters. When the method ran smoothly, a large scale seismic survey was executed.

The reason why small scale surveys and single shot tests were executed was because it is easier to detect errors when the data size is small. There is no point to run a full seismic acquisition with the wrong parameters. Therefore a step by step debug and change of parameter values is the safest way to fix the errors.

The parameters in the processing part was the part that took the longest time to get right. One of the reasons why it took so long time to get the processing right was because many of the parameters were dependent on earlier parameters. Another reason was that there was no consistent parameter value, some parameters needed a value in meters, others needed a grid point value.

After several attempts and numerous hours with debugging and problem solving the result became good (figure 5.7). More work could probably have been done to get the reflections clearer, but a decision to stop working on the processing and rather focus on the interpretation was made.

One way that might lead to a better result would probably be to use another migration algorithm. Kirchhoff time migration is one of the simplest migration algorithms that exists. Most likely would a more advanced migration algorithm like the Reverse time migration and prestack Kirchhoff depth migration give a better result (Arntsen, 2012).

Instead of picking velocities, as in a normal seismic survey, the rms values of the original P-wave velocity model were used as input in the migration. A valid argument against this is that it does not simulate a real seismic process. On the other hand, the migration should in fact work better. The original P-velocity model was one of the models that generated the synthetic seismic. The same model is used to calculate the RMS velocities used in the migration algorithm, hence the RMS velocity can be treated as the correct velocity model. A picked velocity model is expected to be erroneous, because it is based the picks from the semblance plot (Bancroft and Cao, 2004), which corresponds to the velocity with the highest probability (Landrø, 2008).

6.3 The Interpretation

The interpretation of the synthetic seismic (figure 5.9) was not ideally performed. The knowledge of the geological model will interfere with the interpretation of the seismic regardless of the awareness and carefulness shown when interpreting.

A good way to ensure that the interpretation is of a good quality and not affected by the original geological model would be to follow the same method as Johansen et al. (2007). They let an experienced exploration seismologist outside the project interpret their synthetic seismic. Several other seismic interpreters and students also made an interpretation of the synthetic seismic. This gives a good overview of the most likely way to interpret the seismic.

This was not done in this study, but it would be a good way to ensure that the interpretation would not be affected by any knowledge of earlier processes. No one outside the project interpreted this seismic, but support and quality check of the interpretation was given by fellow students.

6.4 Data Quality

The overall quality of the seismic line is good, but there are some areas in the seismic line (figure 5.7) that have poor data quality. The area marked in figure 6.1 is the part where it is most noticeable. One possible answer to this artefact is that it is generated when migrating the data. The source of this visualization problem may lie far back as the creation of the structured grid, which is used to build the model in Petrel.

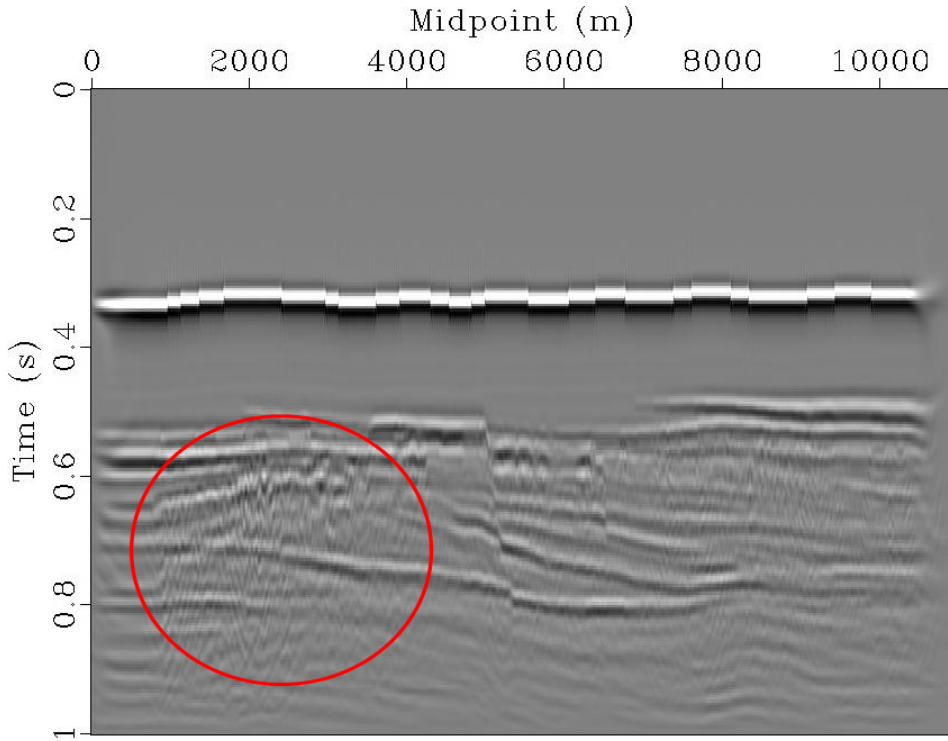


Figure 6.1: The data quality inside the red circle is obscured, most likely caused by the processing flow. The entire data is a bit obscured but it is most noticeable inside the red circle.

The structured grid used in the building of the model is like in figure 6.2. When the values from a dipping layer get assigned to the grid model, the boundary between two layers may look like the red line. All the grid points above the line are one layer, the ones beneath, including the ones the line cuts, are another layer. When the data is acquired, these sharp edges and the stepwise boundary in the property models might cause diffraction of the signal.

During the migration, the data caused by diffraction, might be enhanced and be the reason for the distortion of the signal inside the red circle in figure 6.1. It is worth to notice that the areas with the most distortions are those in an area with several very thin dipping layers (see figure 4.1). The vertical shifts in the seabed are most likely caused by the grid in the model.

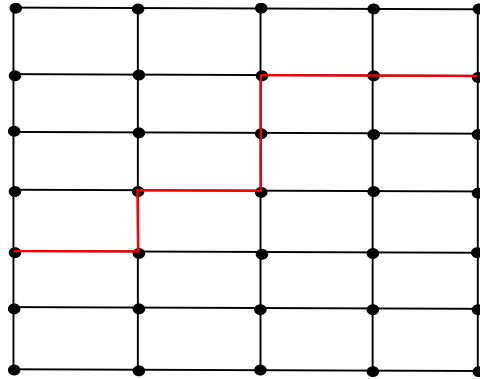


Figure 6.2: The problem with the grid is that when a layer is dipping, the boundary between the two layers may look like the red line. This may cause diffraction in the seismic acquisition and result in the bad data in the figure 6.1.

If the grid size had been smaller, the representation of a dipping layer might have been a bit smoother, which may cause less diffraction. However, too small a grid step size might cause the accuracy on the seismic modeling algorithm to decrease, due to round off errors (Krebs, 2004). Another possible explanation, but less probable, is that the disturbance is caused by an instability in the migration.

If figure 5.7 is compared to the bottom image in figure 6.3, it looks like the data quality is a bit better in figure 6.3, this is probably due to the scale. In figure 5.7 the picture is almost quadratic and in figure 6.3 it is rectangular. In reality (figure 4.1) the model is about 10000×1000 m, which is 10 times as long as it is deep. That might explain that the bottom image in figure 6.3 looks like have better quality.

6.5 Comparison of the Synthetic Seismic and the Geological Model

The seismic forward realization uses figure 4.1 as an input and ends up with figure 5.7. An interpretation of the seismic line is shown in figure 5.8. The geological model and the seismic line are also displayed in figure 6.3 (a larger picture in Appendix A figure A.11) and some similarities can be seen, but also some differences, especially on the left side.

In figure 6.3 the seabed is very clear and is easily mapped (A), which is expected because it is the first reflector and the signal strength is still high. The rest of the model can be divided into three parts: the left, the middle and the right part. The faults from figure 4.1 are the lines that divide the model.

Those reflections on the right hand side (B-H, N and O) are most likely to be strong and clear because of the simple layering with a large velocity contrast and with almost no small thin layers. Many small thin layers may generate many internal multiples, which interfere with the seismic signal. In this area the seismic reveals almost every layer. The only exceptions are some layers above layer H. All these layers are very thin, so the wavelet

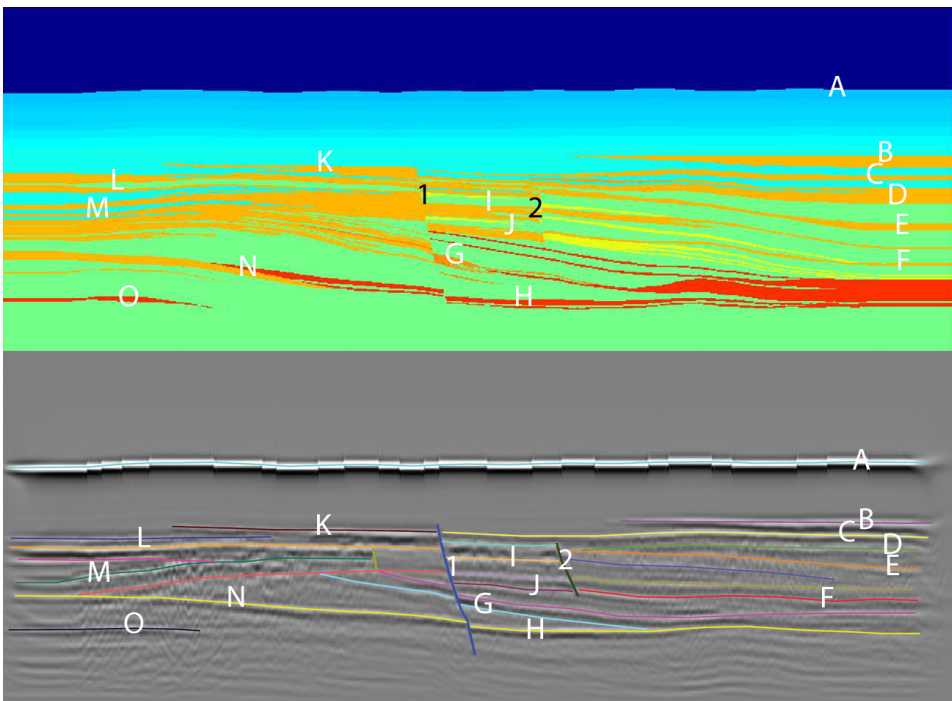


Figure 6.3: Comparison between the geological model displayed at the top by the property model of the p-wave velocity (figure 4.1) and the interpret synthetic seismic (figure 5.8). The horizons marked with the same letter are interpreted as the corresponding layers. The numbers correspond to faults. See appendix A figure A.11 for a larger picture.

might not detect them all. The top of the large red (turbidite) layer is not clearly visible. It may be the interpreted layer beneath layer F. The yellow delta front layer above the turbidite layer may cause the contrast to be weak and that might be the reason it does not show.

In the middle part, between fault 1 and 2, there are many thin layers at the top that do not show up on the seismic. The ones that show up (I and J) are those layers that are fairly thick with a high velocity contrast (about $500 \frac{m}{s}$).

On the left hand side the top interpreted layers (K-M) might be traced back to the original model. The layers in this area, are thick without many thin layers in between. It is not completely clear which layer the interpreted layer M corresponds to in the geological model, mostly because of the noise in the data. Beneath layer M there are some thin layers, which may cause the obscurity in the data. Beneath the obscure data, layers N and O are visible. These are high velocity contrasts (about $1000 \frac{m}{s}$) but not very thick.

Figure 5.10 is the picture interpreted while looking at the geological model. By comparing this figure with figure 5.8, it is possible to see which layers that are placed at its right position. The smallest fault to the left has been removed together with some layers on the left side, in the noisy area. Also some layers down right have been moved, edited and

some new ones have been added to better fit the geological model. It can be seen that the top and bottom layers together with the top middle fit very well with the geological model.

The letters (A-O) in figure 6.3, show almost the same layers as figure 5.10. The only difference is there are some difference above layer H and below layer F.

Conclusion and Recommendation

7.1 Conclusion

This work has shown that it is possible to do forward seismic modeling by building property models in Petrel, starting with a picture of the geological model. The picture was digitized and property models were built. These models were used as input into an open source software called Madagascar, which predicts the responses from the subsurface. The software solves the center finite difference discretization of the elastodynamic equations using the models as input. The source wavelet was a Ricker wavelet with a maximum frequency of 100 Hz.

The seismic shots were processed using a very simple flow, with a 2-D Prestack Kirchhoff time migration with anti-aliasing as the migration algorithm. The resulting seismic line was of good quality, except an area which is thought to contain a lot of diffraction caused by the grid.

The interpretation of the seismic line could see almost all of the thick layers with a high velocity contrast. In areas with several thin layers with shifting velocities, the seismic was blurred and it was not possible to detect the individual layers.

7.2 Further Work

This thesis uses a 2-D dataset, for further work 2.5-D models might be used to simulate a 3-D seismic survey and processing. This will result in a seismic cube which should be converted to Petrel files for interpretation.

It would be interesting to see if a more advanced processing flow would enhance and clean the seismic. Like for instance, how a prestack depth migration algorithm would migrate the data compared to the 2-D Prestack Kirchhoff time migration. In order to simulate a more realistic processing flow, the velocity model used in the migration should have been picked using a velocity analysis instead of the same velocity model as in the seismic acquisition.

Bibliography

- Alaei, B., 2012. Seismic modeling of complex geological structures. In: Kanao, M. (Ed.), Research and Analysis [Online]. InTech, pp. 213–336, available from: <http://www.intechopen.com/books/seismic-waves-research-and-analysis/seismic-modeling-of-complex-geological-structures> [Accessed April 16, 2013].
- Anderson, N., Cardimona, S., 2002. Forward seismic modeling: The key to understand reflection seismic and ground penetrating radar (gpr) techniques.
- Arntsen, B., 2011. Geophysical Analysis lecture Notes. Norwegian University of Science and Technology.
- Arntsen, B., 2012. Reservoir Seismics Lecture Notes. Norwegian University of Science and Technology.
- Bancroft, J. C., Cao, Z., 2004. A comparison of cmp and eo gathers for multiple-attenuation. CSEG National Convention.
- Buckley, S., Schwarz, E., Terlaky, V., Howell, J., Arnott, R., 2009. Terrestrial laser scanning combined with photogrammetry for digital outcrop modelling. IAPRS XXXVIII (3), 75–80.
- Dallmann, W., 2009. Svalbards geological development [online]. Norwegian Polar Institute, available from: <http://cruise-handbook.npolar.no/en/svalbard/geological-development.html> [Accessed January 15, 2013].
- Johansen, S., Granberg, E., Mellere, D., Arntsen, B., Olsen, T., 2007. Decoupling of seismic reflectors and stratigraphic timelines: A modeling study of tertiary strata from svalbard. *Geophysics* 72 (5), 273–280.
- Johnsen, S., Mørk, A., Dypvik, H., Nagy, J., 2001. Outline of the geology of svalbard. 7th ESF IMPACT Workshop.
- Krebs, E. S., 2004. Seismic forward modeling. *CSEG Recorder* April, 28–39.

-
- Landrø, M., 2008. Anvendt geofysikk i TPG4100 Fysikk og Geofysikk. Norwegian University of Science and Technology, [In norwegian].
- Landrø, M., 2011. Seismic Data Acquisition and Imaging. Norwegian University of Science and Technology, Trondheim.
- Madagascar, 2013. Madagascar homepage [online]. Available from: <http://www.ahay.org/> [Accessed May 15. 2013].
- Pringle, J., Howell, J., Hodgetts, D., Westerman, A., Hodgson, D., 2006. Virtual outcrop models of petroleum reservoir analogues: a review of the current state-of-the-art. First Break 24, 33–42.
- Schlumberger, 2013. Schlumberger homepage [online]. Available from: <http://www.slb.com/> [Accessed May 16. 2013].
- SCM, 2011. Petrel tips & tricks from scm: Import and digitize from a bitmap using petrel. Available from: http://www.scminc.com/port/SCM_Scan_Register_Digitize_Bitmap_Petrel_2010.pdf [Accessed May 15. 2013].
- Virieux, J., 1989. P-SV wave propagation in heterogeneous media: Velocity-stress finite-difference method. Geophysics 51 (4), 889–901.

Appendix

Appendix A - Pictures

The following pictures in this appendix are:

- A.1 P-velocity model built in Petrel - Large picture of figure 2.6
- A.2 S-velocity model built in Petrel
- A.3 Density model built in Petrel
- A.4 Converted P-velocity model - Large picture of figure 3.2
- A.5 Converted S-velocity model
- A.6 Converted density model
- A.7 Resized model - Large picture of figure 4.1
- A.8 Interpret Seismic - Greyscale - Large picture of figure 5.8
- A.9 Interpret Seismic - Red-white-blue - Large picture of figure 5.9
- A.10 Interpret Seismic - Large picture of figure 5.10
- A.11 Model versus synthetic seismic - Large picture of figure 6.3

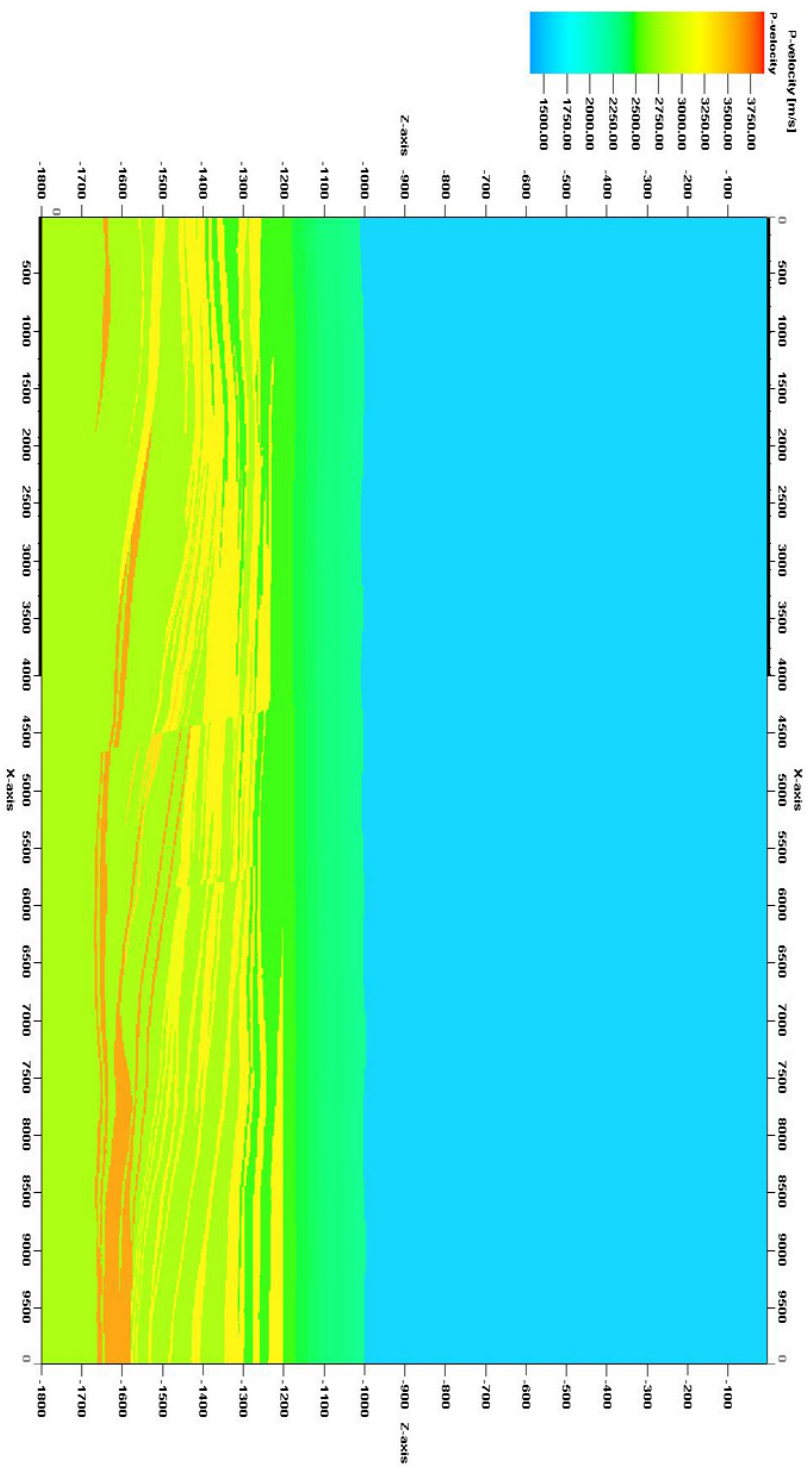


Figure A.1: P-velocity model built in Petrel. The property model from Johansen et al. (2007) (figure 2.3) has been flattened at the top right yellow sandstone, and buried beneath 1000m of seawater and 200m of shale. This model can be used as an input in seismic forward modeling.

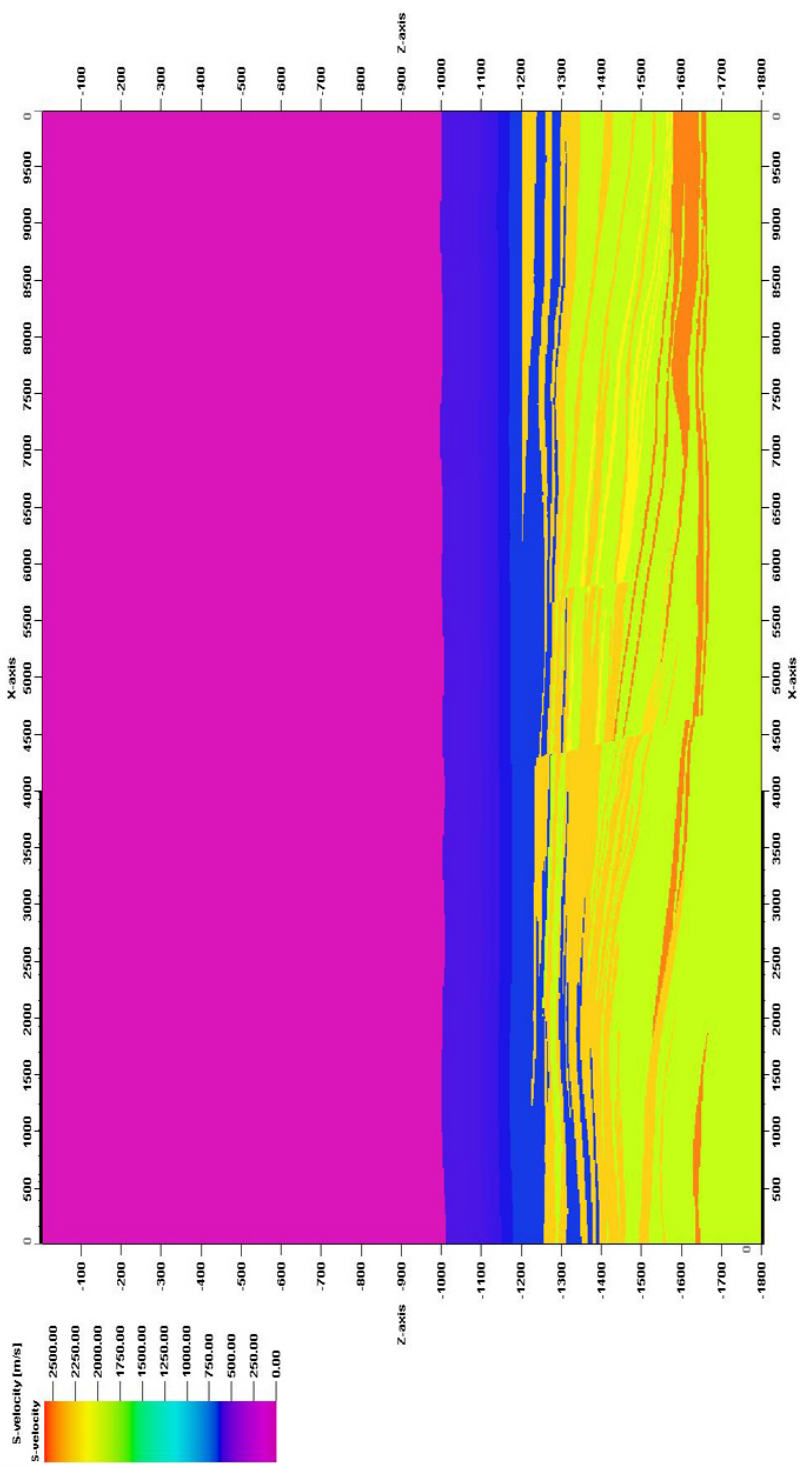


Figure A.2: S-velocity model built in Petrel. The property model has been flattened at the top right sandstone, and buried beneath 1000m of seawater and 200m of shale. This model can be used as an input in seismic forward modeling.

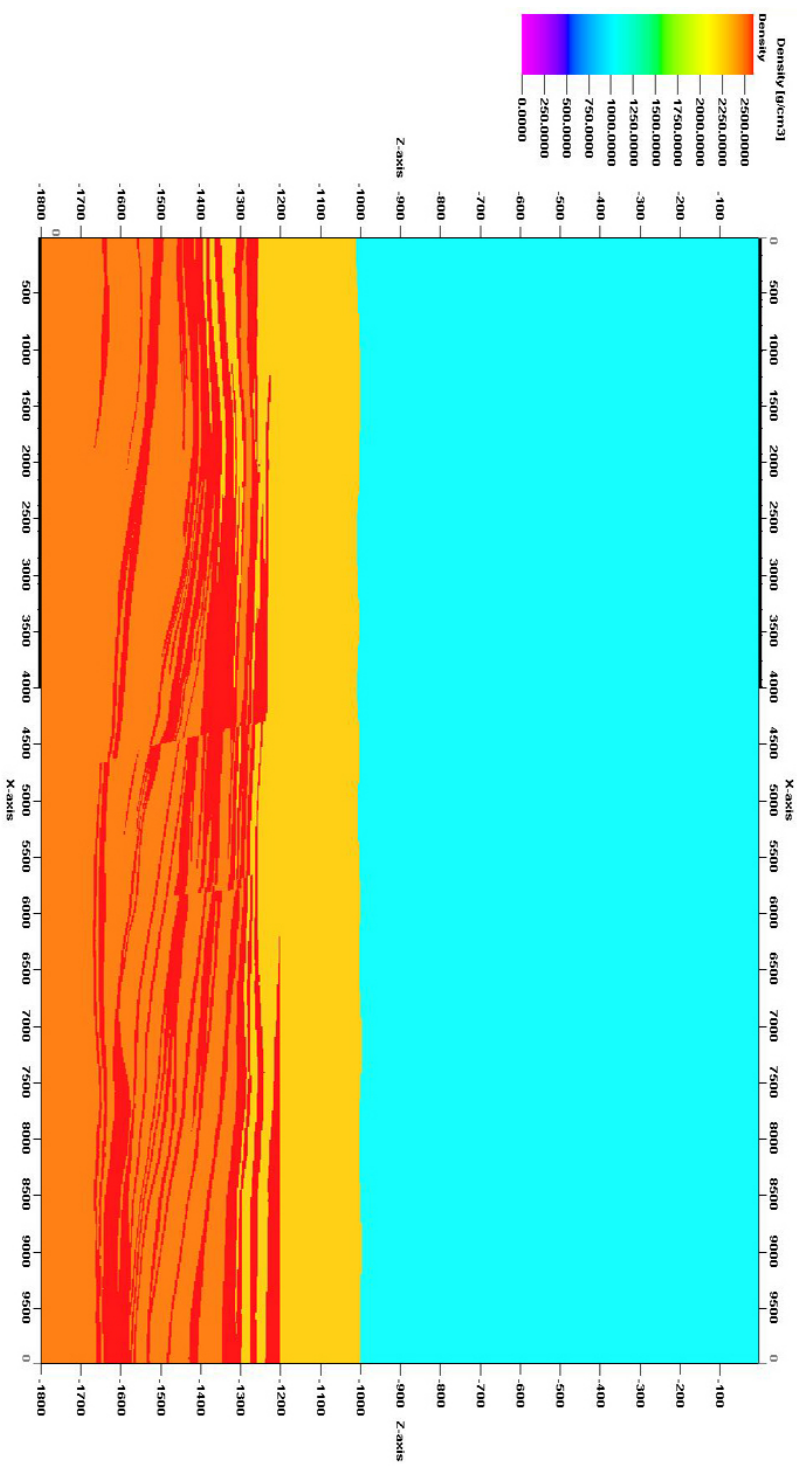


Figure A.3: Density model built in Petrel. The property model has been flattened at the top right sandstone, and buried beneath 1000m of seawater and 200m of shale. This model can be used as an input in seismic forward modeling.

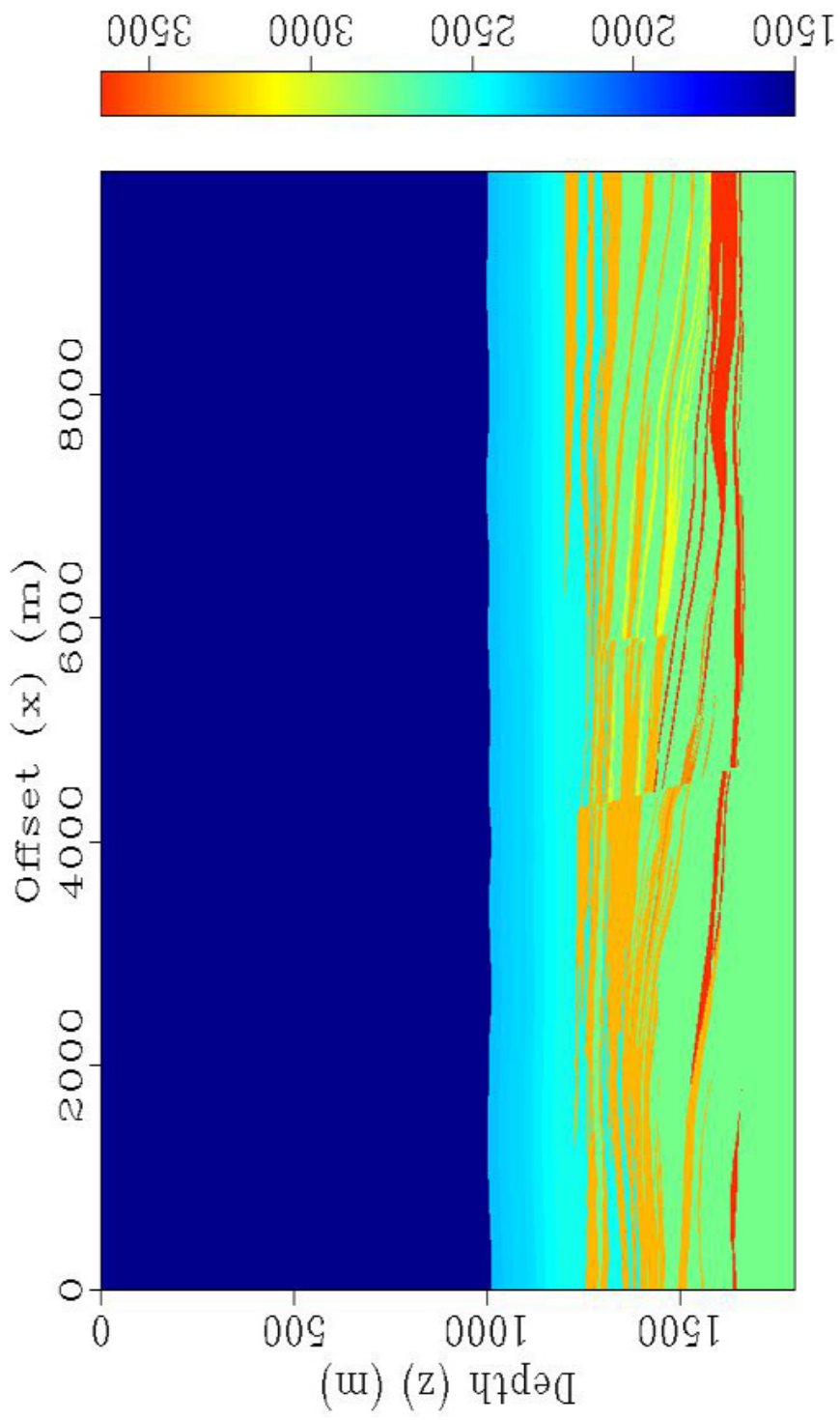


Figure A.4: Converted P-velocity model from Petrel through ECLIPSE to Madagascar.

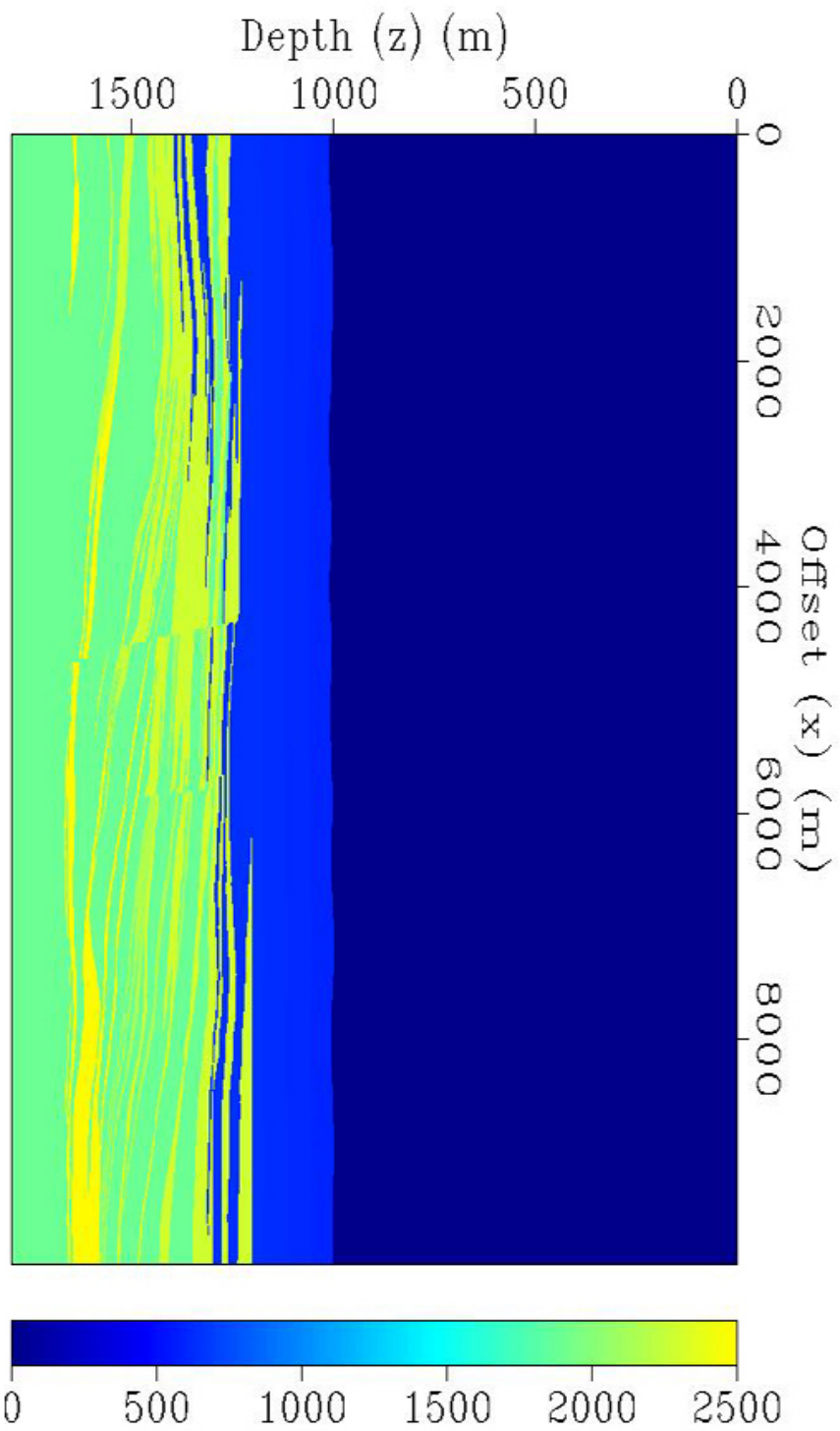


Figure A.5: Converted S-velocity model from Petrel through ECLIPSE to Madagascar.

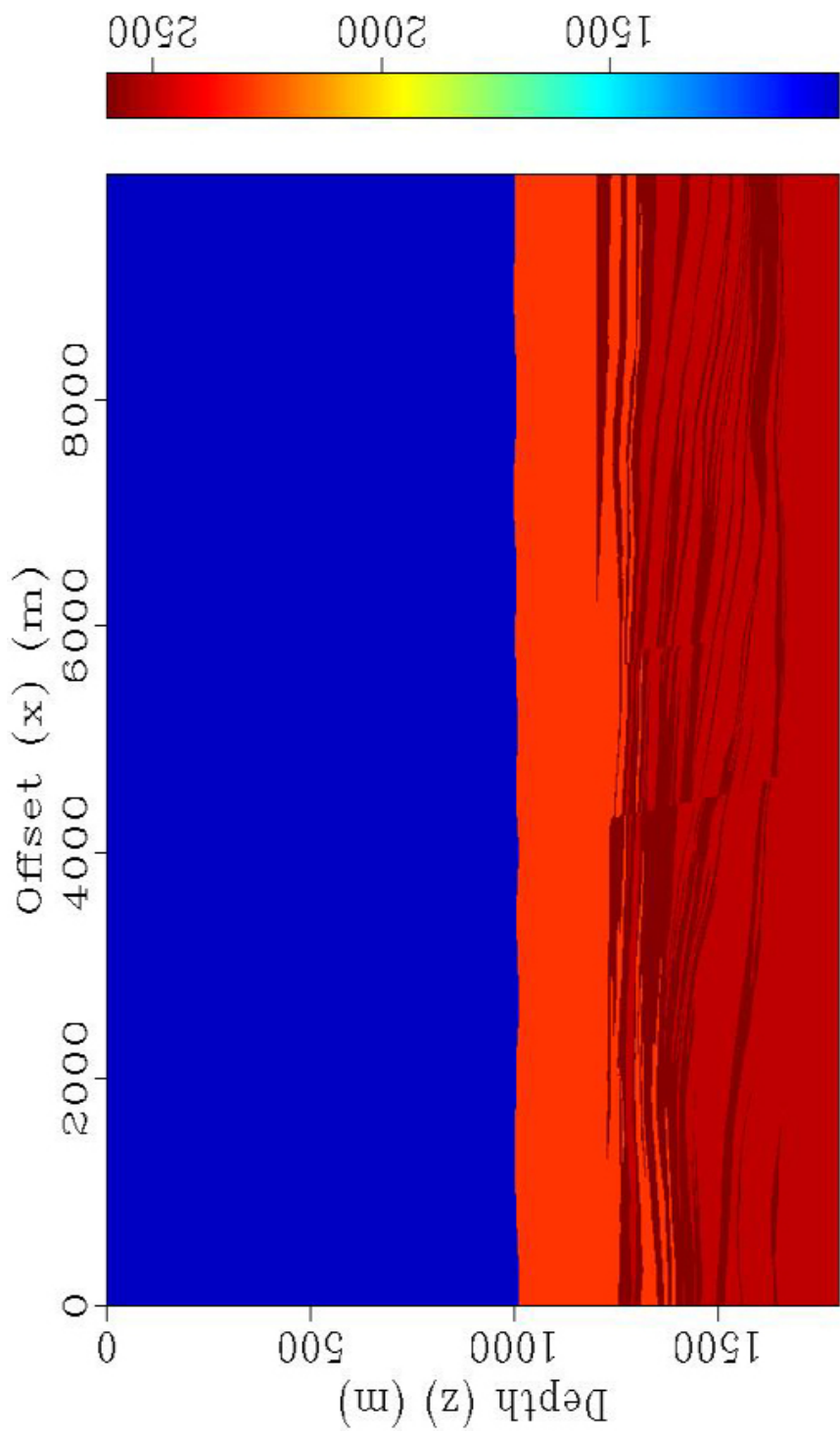


Figure A.6: Converted density model from Petrel through ECLIPSE to Madagascar.

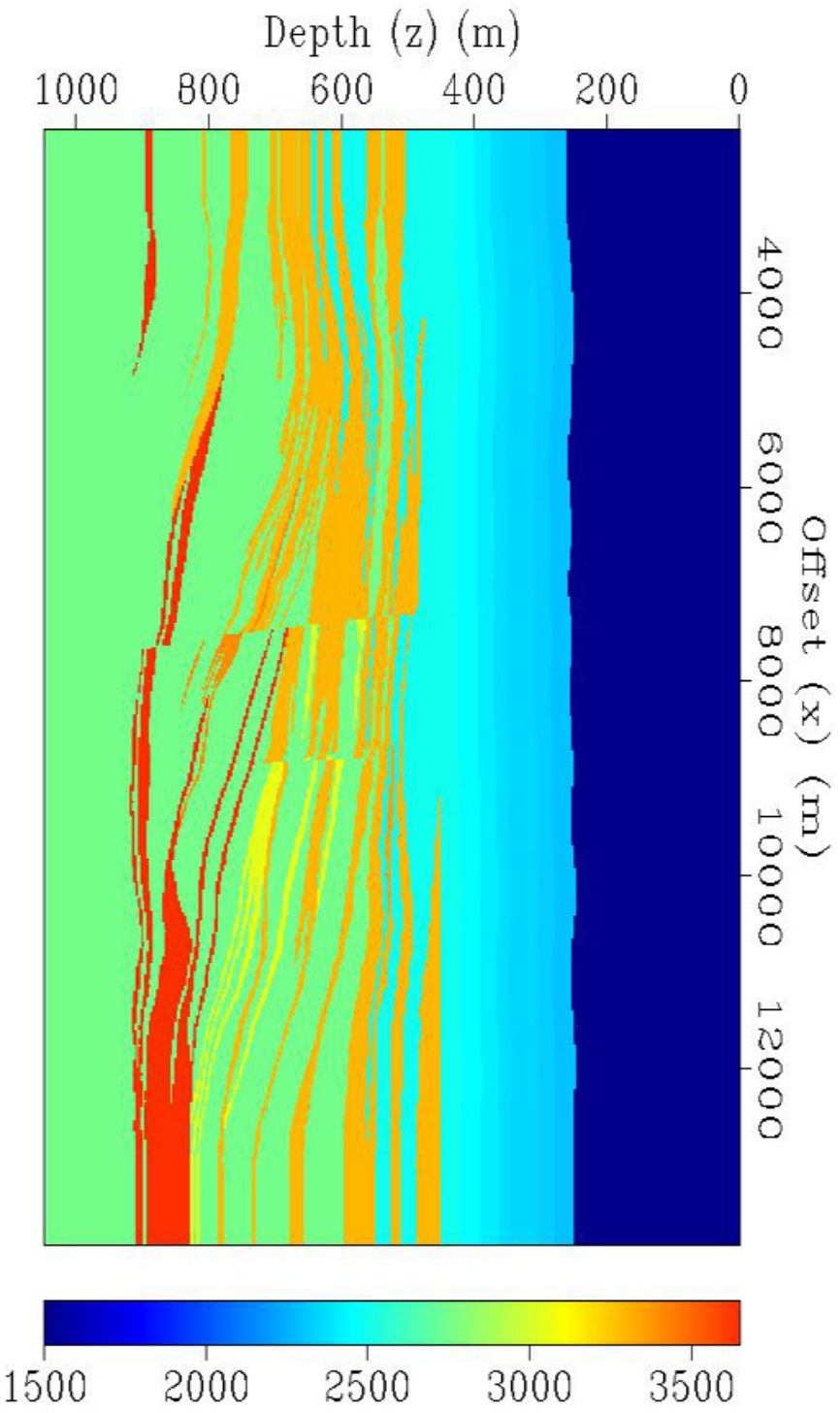


Figure A.7: The same figure as figure A.4 but this has been cut. The top 750 meters has been removed because of the free surface parameter in the Madagascar software. The model has also been extended on both sides, this to get full fold over the entire area of interest when acquire the seismic. The same has been done to the density and S-velocity models.

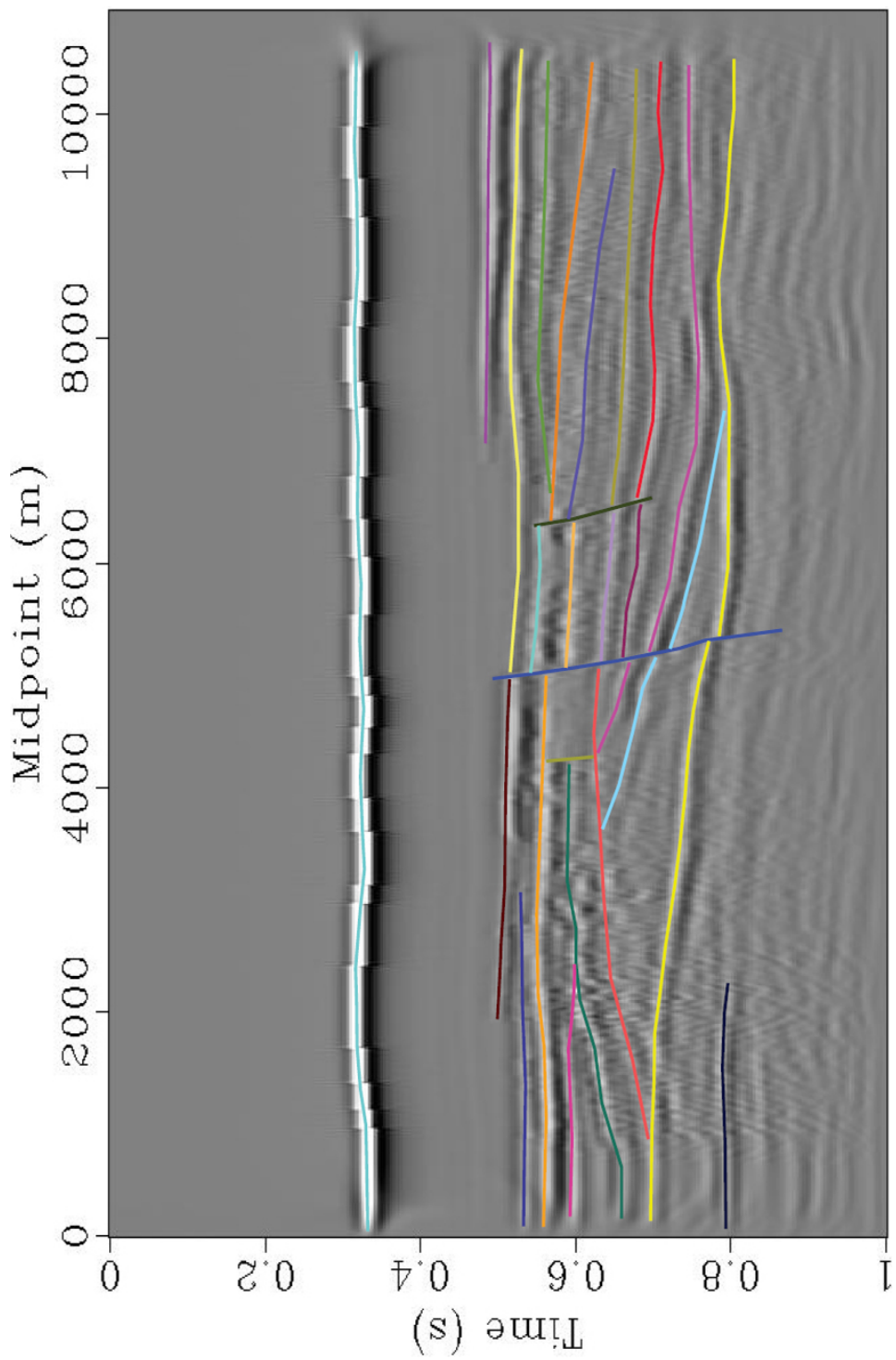


Figure A.8: Interpretation of the synthetic seismic using a greyscale color mapping.

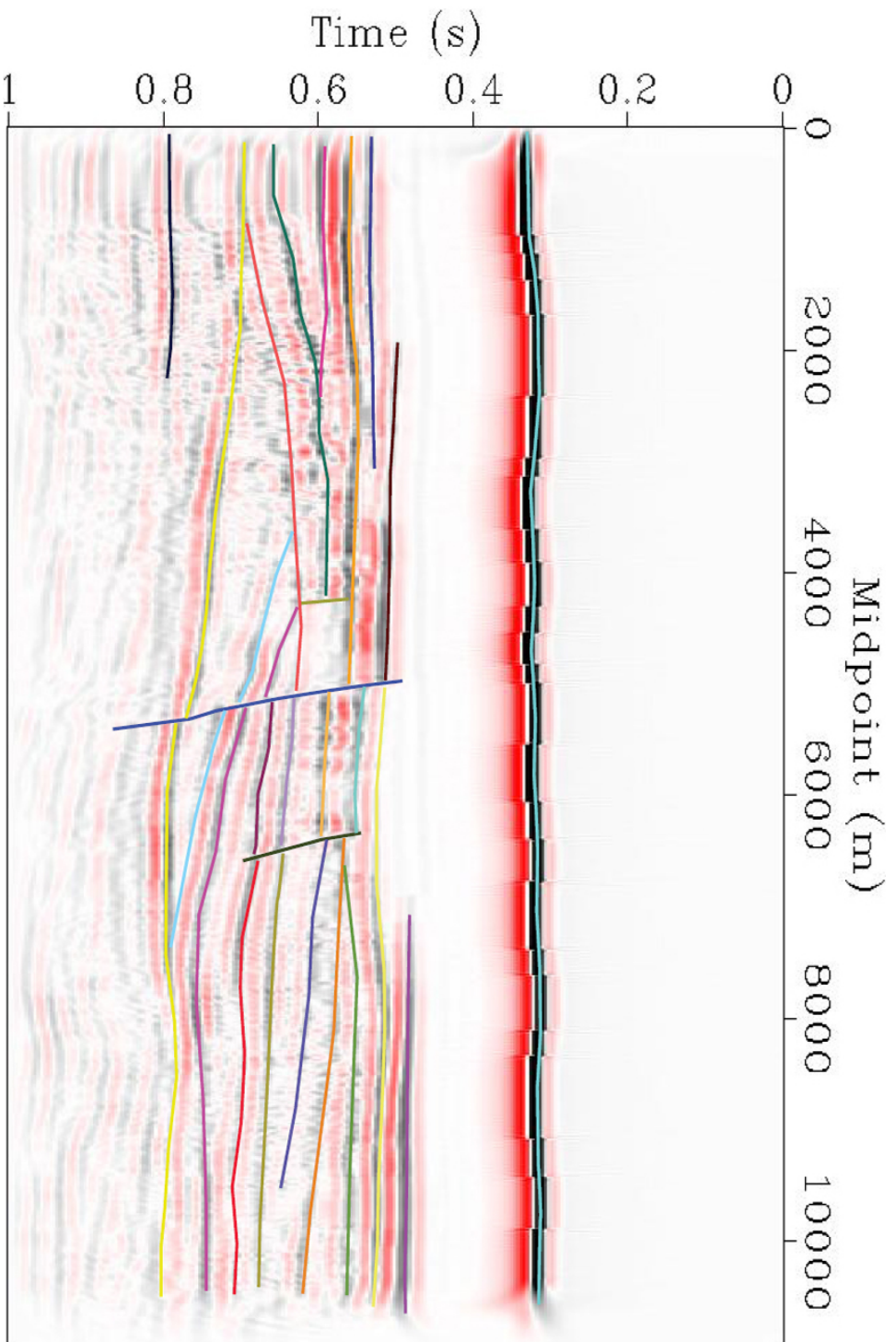


Figure A.9: Interpretation of the synthetic seismic using a red-white-blue color mapping.

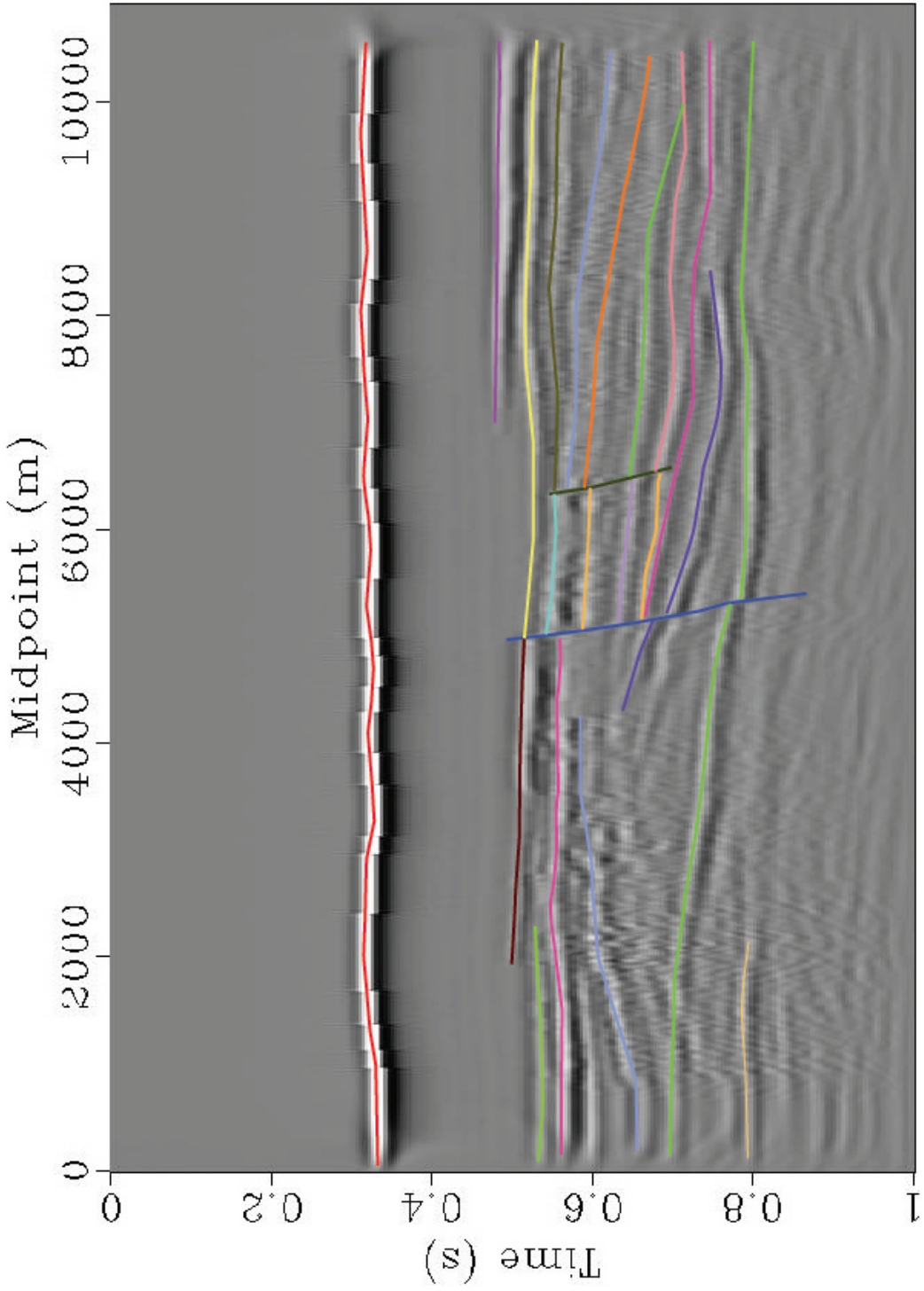


Figure A.10: Interpretation of the visible layers in the geological model on the synthetic seismic.

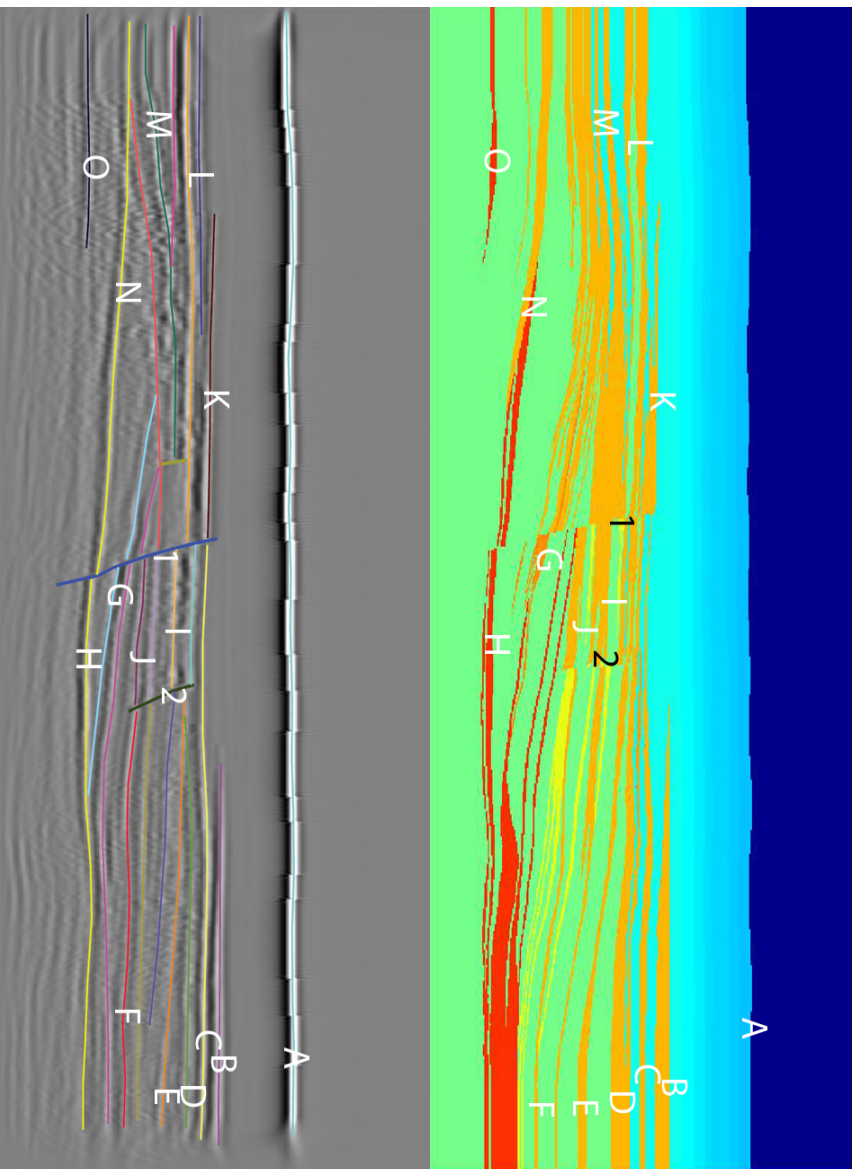


Figure A.11: Comparison between the geological model displayed at the top by the property model of the p-wave velocity (figure 4.1) and the interpret synthetic seismic (figure 5.8). The horizons marked with the same letter are interpreted as the corresponding layers. The numbers corresponds to faults.

Appendix B - Model building in Petrel

When building a model in Petrel out of a picture, like figure B.1, the *Surface imaging* module needs to be available. This module makes it possible to assign coordinates and locate the picture in the world.

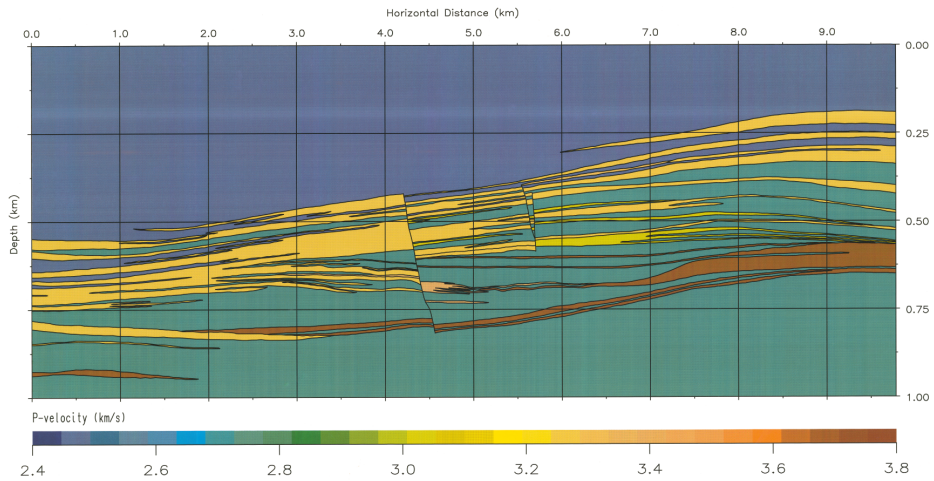


Figure B.1: V-velocity model of Storvola, used as input in Petrel and the model building (Johansen et al., 2007).

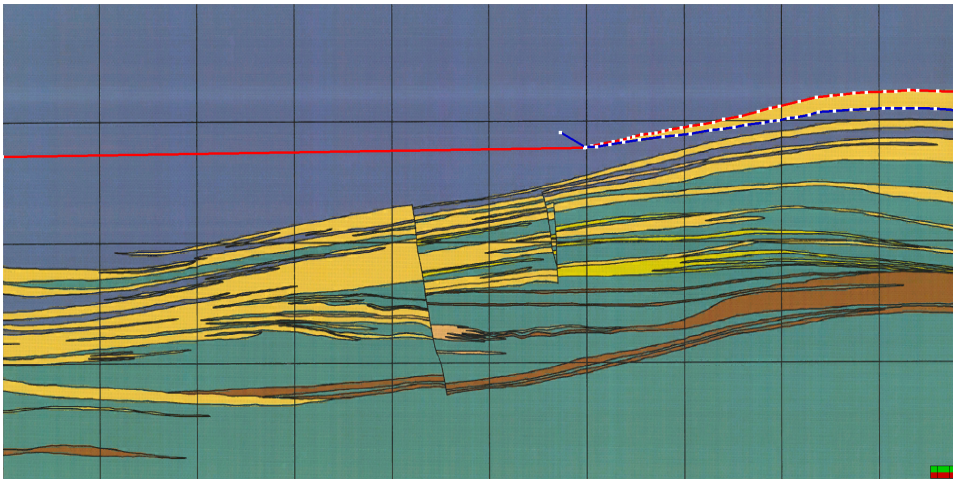


Figure B.2: Mapped layer in Petrel, using the process *Make/edit polygons* on the picture.

The process *Make/edit polygons* is used to select points along a horizon on the picture (figure B.2). Petrel automatically uses linear interpolation between the picked points.

These polygons can be converted into a surface by the use of the process *Make/edit surface*.

In the make/edit surface process it is necessary to decide the boundaries of the surface and the algorithm to convert the polygons with. In this work the algorithm closest is used (figure B.3, left). After the generation of a surface (figure B.4), it is necessary to do smoothing. Smoothing is done to remove sharp edges the algorithm has generated when converting the polygon to a surface (figure B.3, right).

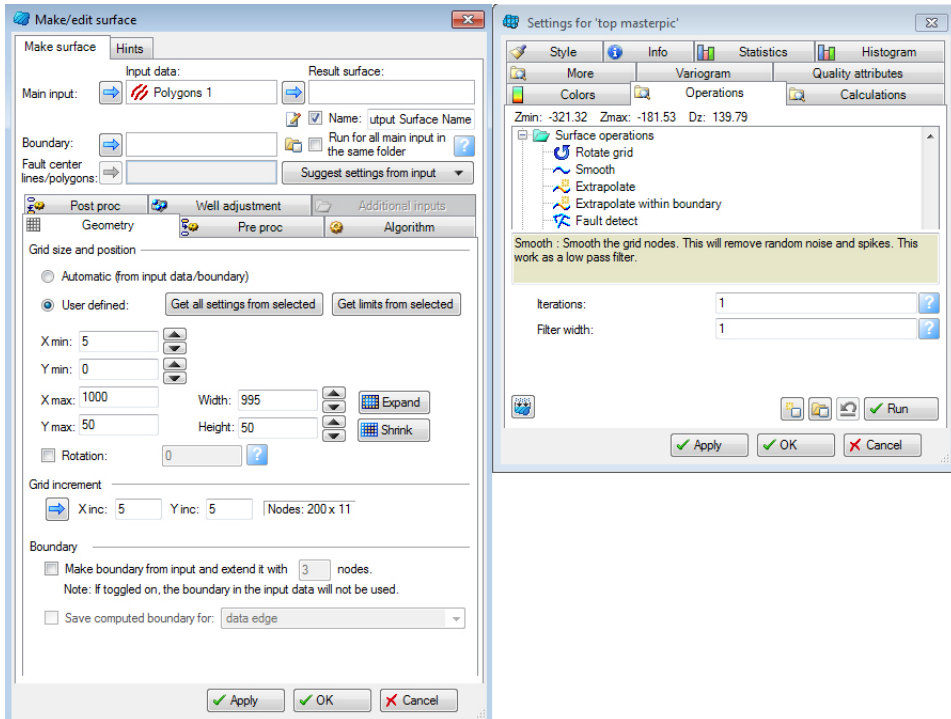


Figure B.3: The left figure is the *Make/edit surface* process were the polygons are converted to surfaces. After generating a surface the surface has lots of sharp edges, which are removed by smoothing (figure to the right).

It is also possible to move surfaces, and this was done to flatten the model. To do this, a difference surface was generated, which is a mathematical surface, not a geological surface. This surface vary according to the amount the flattening surface needs to be corrected to become horizontal. The difference surface could now be added to every surface, which would move the surfaces according to the flattening (see figure B.5).

After all the surfaces has been mapped, it is time to build a property-model. The process *Make simple grid* may be used to build the boundaries and the grid of the model. The only values required are the depth, length and width of the model and the grid size in the x (length) and y (width) direction. The grid size in the z (depth) direction needs to be determined in the *Layering* process, by dividing the zone into the number of layers desirable (it should only be one zone there).

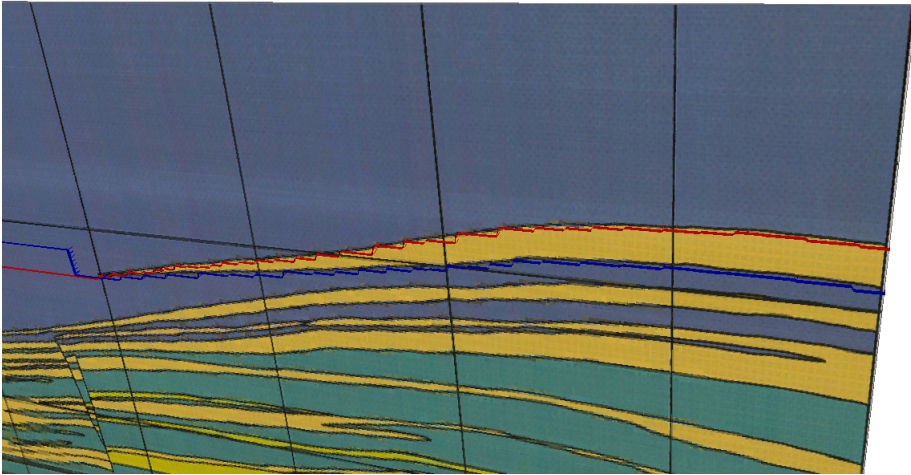


Figure B.4: A generated surface from the process *Make/edit surface*.

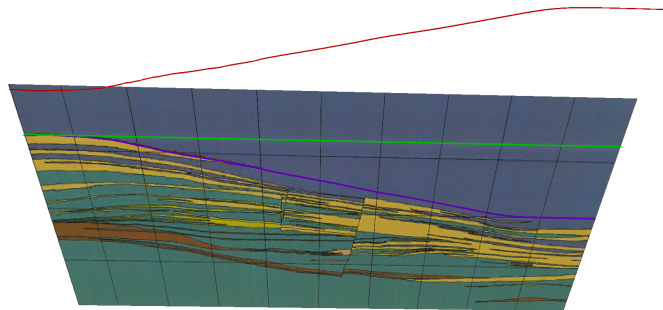


Figure B.5: The purple surface is the surface called the flattening surface. The green surface is the horizontal surface, which intersects the flattening surface at its minimum point. The flattening surface should look like the green surface after its flatten. The red surface is the difference surface, which is the difference between the purple and the green surface.

Before assigning values to the models, it is necessary to set the surfaces equal to each other in some areas. To do this some modification to the surfaces need to be performed, and to do this a surface calculator is used (figure B.6, left). The final result may be seen in figure B.7.

The model is now ready to be assigned values. The process used is the one called *Geometrical modeling*. The method used is assigning values between surfaces, which require the input of two surfaces, one top and one base. The value to assign between the surfaces also needs to be decided (figure B.6, right). It is also possible to assign a value outside the area between the surfaces, however, this is generally not used, except when assigning values for the first time. It is a good idea to assign a value outside the area between the surfaces that cover much of the area in the model and is hard to map, like for

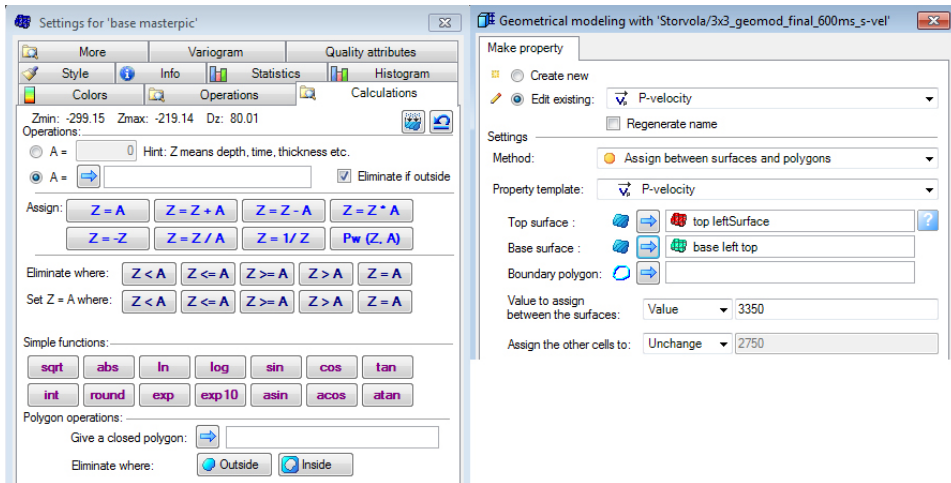


Figure B.6: The surface calculator is used to set surfaces equal to each other in areas where this is desirable (left figure). The right figure is the geometrical modeling process, which is used to assign properties between two surfaces.

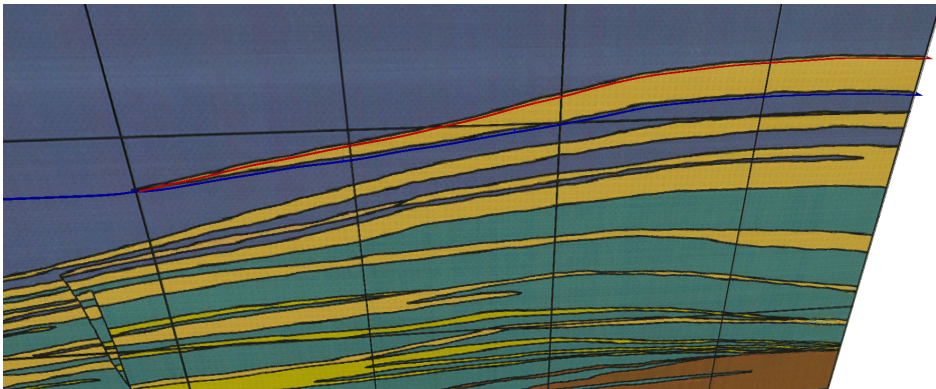


Figure B.7: The final surfaces, which are equal outside the area of the yellow sandstone. These surfaces are used as input in the *geometrical modeling* process.

instance the dark green color in figure B.1. This is handy because it is easy to overwrite this value later by "real" values and this also assures that all the grid points get assigned a value, in case the surfaces do not manage to fill them all.

After all properties have been inserted into the model, the result may look something like figure B.8. For figure B.8 the surfaces have also been buried beneath 1000m of sea-water and a 200m layer of shale as an overburden. This model, together with a density and a V_s model with similar geometry, may be used in seismic forward modeling.

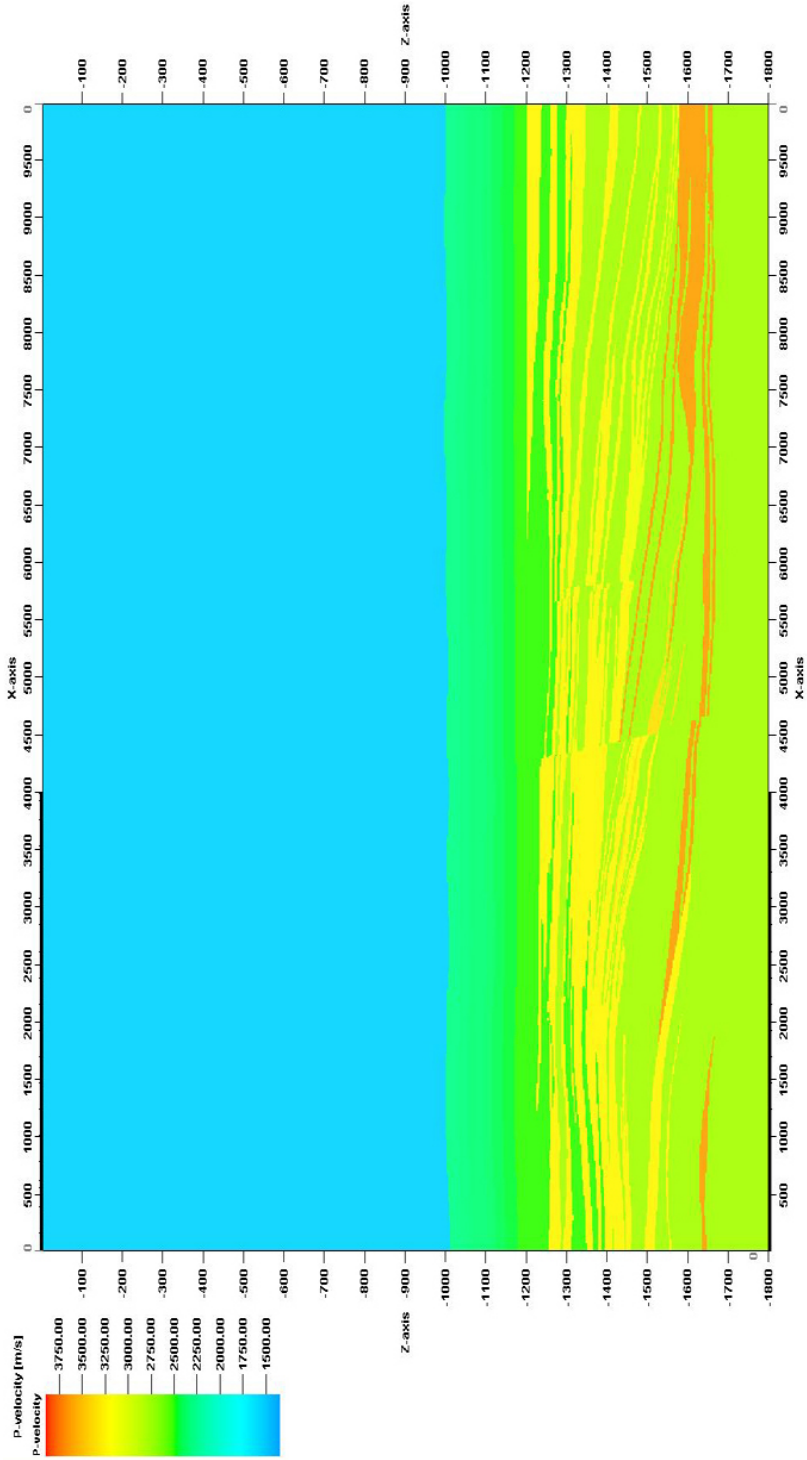


Figure B.8: The V_p -property model built using Petrel. The property model has a 1000m layer with seawater at the top and a 200m layer of shale as an overburden. The structure beneath these layers are the flattened layers in figure B.1. This model can be used as an input in seismic forward modeling together with a similar density and V_s -property model.

Appendix C - Converting a Petrel model to Madagascar

Before it is possible to begin with seismic modeling, it is necessary to convert the Petrel models into a readable file format for Madagascar. Madagascar is an open-source software for multidimensional data analysis and reproducible computational experiments.

Madagascar uses a simple file format called Regularly Sampled Format (RSF). The RSF file consists of a header and a binary part often separated into two files. The header file is an ASCII text file (readable for humans) with suffix `.rsf` and is usually stored locally. This file contains the attributes of the RSF like the maximum and minimum value. The binary part is usually stored in a separate directory with suffix `.rsf@`, and it is the binary file that contains all the data.

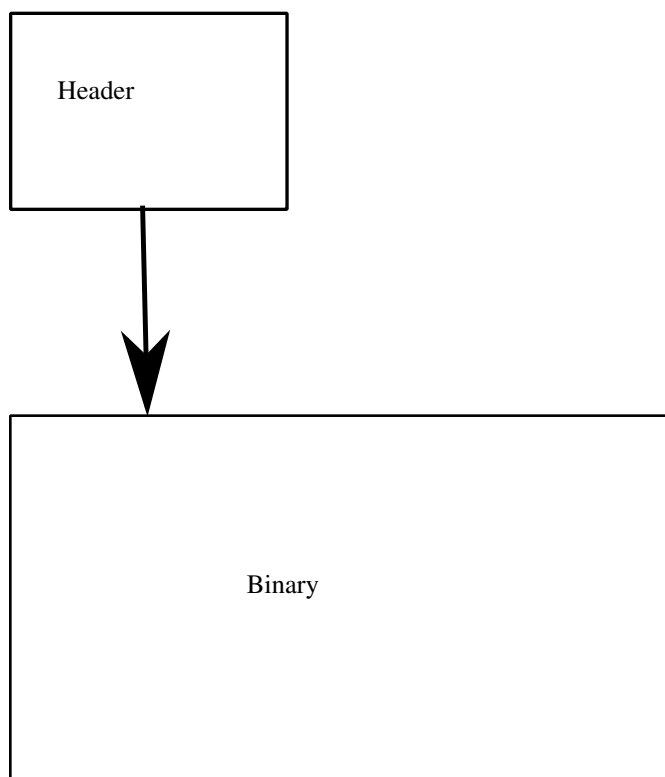


Figure C.1: Illustration of the RSF file format. The header file points to the binary file, which contains the data. The header file contains the attributes of the RSF that can be read by humans (from Madagascar (2013)).

The property models built in Petrel can not be exported to the RSF file format directly. The way it is done is that first the models are exported to ECLIPSE files. ECLIPSE is mainly a reservoir simulation tool own by Schlumberger, who also own the rights to Petrel. Schlumberger (2013) describe ECLIPSE like this: *"ECLIPSE is a numerical solution for fast and accurate prediction of dynamic behavior for all types of reservoirs and degree of*

File Name	File Type
<i>vp</i>	GRDECL File
<i>vp_ACTNUM</i>	GRDECL File
<i>vp_COORD</i>	GRDECL File
<i>vp_PROP_P – VELOCITY</i>	GRDECL File
<i>vp_ZCORN</i>	GRDECL File

Table C.1: The converted Petrel files, where *vp* is a header file, and the four others contain the model geometry and property values.

complexity, structure, geology, fluids and development schemes.”

Because the ECLIPSE software is connected to Petrel it is possible to export Petrel models into ECLIPSE format and do simulations on the models. In this case, the ECLIPSE format is just the first stop when converting the models.

For converting the Petrel model go to the *Models pane* and right click on the model to convert and choose *Export*. In the window that now appear choose save as *ECLIPSE keywords (grid geometry and properties (ASCII))* and give the files a name and then save. In the next window that appear choose the properties to export and hit OK.

When finished there should be five .GRDECL files (table C.1). The *vp.GRDECL* is a header file that links all the ECLIPSE files together, the other four contain the geometry and the property values.

When the ECLIPSE files have been made, a method in the Madagascar software called *sfpetread* is used to convert the ECLIPSE files into RSF files. The code to convert the model look like this:

$$sfpetread > vp.rs\ petfile = vp.GRDECL$$

where *vp.rs* is the output RSF file.

The version of *sfpetread* used in this work was case sensitive and it was necessary to configure some of these files by changing the *P-velocity* to *Facies* (this might have been changed).

The P-velocity model in figure C.2 is the output from the conversion and is readable for the Madagascar software.

This recipe is repeated for both the density model and the P-velocity model.

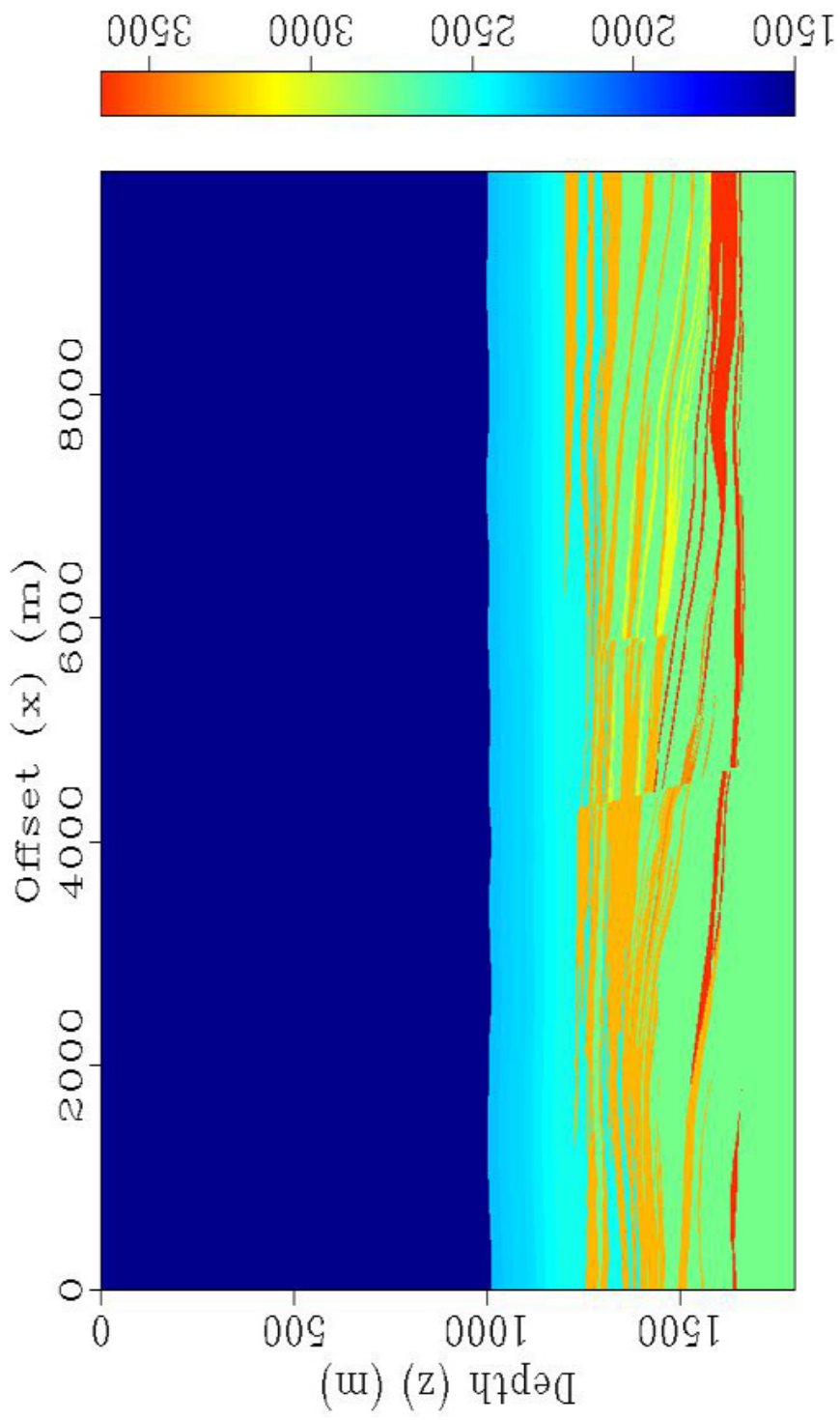


Figure C-2: Converted p-velocity model from Petrel through ECLIPSE to Madagascar.

Appendix D - Seismic Acquisition

The following script is the SConstruct file used to acquire the synthetic seismic data, with some comments on why the process is done. A template of the flow was given to me by *Espen Birger Raknes*, a Phd Candidate at NTNU.

```
from rsf.recipes import msimmod
from rsf.proj import *

### Span the model
Flow('rho-span', 'dens', 'span axis=2 n=1000 place=1 | span axis=2 n=1000 place=2');
Flow('vp-span', 'vp', 'span axis=2 n=1000 place=1 | span axis=2 n=1000 place=2');
Flow('vs-span', 'vs', 'span axis=2 n=1000 place=1 | span axis=2 n=1000 place=2');
```

The extension of the model is done to get full fold over the entire model. That is why 1000 grid points are added on both sides of the original models.

```
### Cuting models
Flow('rho-cut', 'rho-span', 'window f1=250');
Flow('vp-cut', 'vp-span', 'window f1=250');
Flow('vs-cut', 'vs-span', 'window f1=250');
```

```
### Shift Orgin
Flow('fin-rho', 'rho-cut', 'put o1=0');
Flow('fin-vp', 'vp-cut', 'put o1=0');
Flow('fin-vs', 'vs-cut', 'put o1=0');
```

The 250 grid points at the top of the model are removed. That us because all these represent the water, and the idea when building the model was to have a thick water layer so that no sea floor multiples interfere with the data. After studying the modeling algorithm, the method had a free surface parameter which do not give reflections at the sea surface. The origin also needed to be shifted so that the geometry would be correct.

```
### Resampling models
# Flow('rho-re', 'rho-cut', 'window j2=3 j1=3');
# Flow('vp-re', 'vp-cut', 'window j2=3 j1=3');
# Flow('vs-re', 'vs-cut', 'window j2=3 j1=3');
```

If a re-sample is necessary the above method can be used, but it was not used for this acquisition.

```
### Modeling
# Parameter
par = {
    'dim':2,
    'nshots':864,
```

```
'dt':0.0001,  
'nt':15000,  
'surface':0,  
'local_models':1,  
'ghost_border':65,  
'workingpath': '/work /olepes/'  
}
```

```
par['receiver'] = {'xstart':400,'xend':780,'xinc':2,'z':3}  
par['size']={'nx':800}  
par['inc']={'x':4}  
par['start']={'x':370}  
par['end']={'x':3826}  
par['source']={'x':400,'z':3}
```

```
msimmod.param(par);
```

The acquisition parameters like the cable parameters, source position, sampling interval and the number of shots and some other parameters, are set in the code above.

```
# Wavelet
```

```
msimmod.wavelet('source', 25.0, 500, 1000, par);  
Result('source', 'window max2=1.0 | graph title="Source wavelet"');
```

```
Flow('source-spectra', 'source', 'spectra');
```

```
Result('source-spectra', 'window n1=500 | graph title="Source Spectra"');
```

The generation of the source wavelet, which is a Ricker wavelet with a peak frequency at 25Hz. The source spectra of the wavelet is plotted to see that the Nyquist frequency is met.

```
# Modeling
```

```
msimmod.split('fin-rho', 'fin-vp', 'fin-vs', par);  
msimmod.mod('source', 'fin-rho', 'fin-vp', 'fin-vs', par);  
msimmod.cat('data', par);
```

This is the seismic modeling. First the model is split into local models before the modeling starts by using the *msimmod.mod* function call. At the end all the shot data is combined into one RSF file called *data*.

```
# Plotting
```

```
Result('datagrey', 'data', 'grey');  
End()
```

Appendix E - Processing

The following script is the SConstruct file used to process the data in the thesis, with some comments on what the different functions do. A template of the flow was given to me by *Børge Arntsen*, a professor at NTNU.

```
from rsf.proj import *
```

```
### Resampling
```

```
Flow("shots", "data", "sfwindow j1=40 f1=1000 max1=1.3 | sfput o1=0 o2=0 o3=0 d3=12")
```

The data is re-sampled according to the equation $\Delta t = \frac{1}{2f_{Nyq}}$ and a shift in the dataset is done to remove the delay added in the generation of the wavelet. The origin is moved to keep the geometry correct.

```
### Mute
```

```
Flow("mute", "shots", "sfmutter half=n v0=1650 x0=0 t0=0.1 tp=0.175")
```

The direct wave is removed from the dataset.

```
### Sort to cmp
```

```
Flow("cmps", "mute", "shot2cmp half=n")
```

```
### Convert depth velocity model to time
```

```
Flow("xaa", "fin-vp", "depth2time dt=0.004 nt=300 velocity=fin-vp.rsf")
```

```
### Convert stacking velocities
```

```
Flow("xab", "xaa", "vint2vrms")
```

```
Flow("vrms", "xab", "sfwindow max1=1.2 min2=2310 max2=13818 |  
sfput o2=0 label1='Time units1=s'")
```

The velocity model is converted to time before it is converted to rms values. In the last flow the rms velocity dataset is cut so that the geometry correspond to the area where the waves propagate and the geometry is corrected.

```
### Migration
```

```
Flow("tcmp", "cmps", "transp plane=23 memsize=1")
```

```
Flow('migstack', 'tcmp', 'sfmig2 vel=vrms.rsf half=n')
```

```
Result("migstack", "sfgrey bgcolor=1")
```

The migration algorithm needs its input a certain way, and that is why the CMP dataset is transposed before the migration is done. At the end the migrated data is converted into a picture.
